UNIVERSITÀ
DEGLI STUDI
DI PADOVA

Sede Amministrativa: Università degli Studi di Padova

Dipartimento di Biologia

SCUOLA DI DOTTORATO DI RICERCA IN : BIOSCIENZE e BIOTECNOLOGIE
INDIRIZZO: NEUROBIOLOGIA
CICLO: XXVI

THE ROLE OF CALCIUM HOMEOSTASIS IN MITOCHONDRIAL DISEASES AND NEURODEGENERATION

Direttore della Scuola: Ch.mo Prof. Giuseppe Zanotti
Coordinatore d'indirizzo: Ch.ma Prof.ssa Daniela Pietrobon
Supervisore: Ch.mo Prof. Rosario Rizzuto
Co-supervisore: Dott.ssa Pallafacchina Giorgia

Dottorando: Veronica Granatiero

Ai miei genitori, alla mia famiglia
e a tutte le persone a me care!!!

"La vita è unita se si mette il cuore in quello che si fa, il cuore non come sentimento, ma come desiderio insopprimibile di felicità, di bene, di verità, di giustizia. Quel desiderio che hai sempre e a cui da solo non puoi dare piena risposta….
Ci vuole Qualcosa di più grande per essere liberi. Bisogna che questo Qualcosa di più grande sia un'esperienza, sia Qualcuno presente cui si risponde, sempre, in ogni momento della giornata.
Tutto nella vita deve tendere a quel Qualcosa di più grande!"

(dai Discorsi di Enzo Piccinini)

ABSTRACT

Ca^{2+} is one of the main second messengers of cells and, in particular the Ca^{2+} signaling in mitochondria is involved in different physiological processes spanning from cell metabolism, through the control of mitochondrial respiration and crucial metabolic enzymes, to the response in stress conditions.

Despite the lack of a mechanistic understanding, it is well known that mitochondrial Ca^{2+} overload is the most important trigger for the opening of permeability transition pore responsible for apoptosis induction after several toxic challenges. On the contrary, the role of Ca^{2+} signaling in autophagy only recently started to emerge. Autophagy is a process of self-eating by which cellular organelles and proteins are sequestered and degraded in order to produce energy and amino acids in metabolic stress conditions, such as nutrient deprivation. It is not surprising that mitochondrial Ca^{2+} also plays an important role in the pathological alteration of cell physiology in different human disorders.

In the present work we will consider, in particular, the involvement of mitochondrial Ca^{2+} homeostasis and its correlated metabolic processes in two models of human diseases: mitochondrial disorders and neurodegeneration.

Mitochondrial disorders are a large group of heterogeneous diseases, commonly defined by a lack of cellular energy due to oxidative phosphorylation defects. We used skin primary fibroblasts derived from a patient with a complex I mutation in ND5 subunit, as a model of mitochondrial disorders. This system revealed an interesting correlation between the decrease in mitochondrial Ca^{2+} uptake and the increase in autophagic flux. In addition, our results suggest that this is due to a structural rearrangement of intracellular organelle architecture causing a loss of ER-mitochondria contact sites.

Neurodegeneration is caused by selective and progressive death of specific neuronal subtypes. In order to understand the involvement of mitochondrial Ca^{2+} signaling in the pathogenesis of neurodegeneration, we developed an *in vitro* system of mouse primary cortical neurons and we optimized an *in vivo* model of microinjection in mouse brain regions. In particular, we studied the effect of an increased mitochondrial Ca^{2+} uptake, induced by the overexpression of mitochondrial Ca^{2+} uniporter (MCU, the main responsible of Ca^{2+} entry in mitochondrial matrix), on cell survival, in both primary cultures and in midbrain mouse area. We concluded that mitochondrial Ca^{2+} accumulation induces mitochondrial fragmentation and higher sensitivity to cell death in neurons both *in vitro* and *in vivo*.

RIASSUNTO

Il Ca^{2+} è uno dei principali secondi messaggeri cellulari, ed in particolare il segnale Ca^{2+} mitocondriale è implicato in vari processi fisiologici che spaziano dal metabolismo, attraverso il controllo della respirazione mitocondriale, alla risposta a condizioni di stress.

Nonostante alcuni meccanismi d'azione non siano ancora stati chiariti, il ruolo del Ca^{2+} nell'attivazione del processo apoptotico è ampiamente riconosciuto e comprovato.

Al contrario, il coinvolgimento del segnale Ca^{2+} in un altro importante processo, quale quello autofagico, ha cominciato ad emergere solo recentemente.

Il ruolo del Ca^{2+} a livello fisiologico risulta dunque fondamentale all'interno della cellula e alterazioni nella sua regolazione hanno ripercussioni così profonde da indurre l'evolversi di differenti patologie umane.

Nel presente lavoro verrà approfondito il ruolo del Ca^{2+} mitocondriale in particolar modo in due modelli di patologie umane: le malattie mitocondriali e la neurodegenerazione.

Le malattie mitocondriali sono un gruppo molto eterogeneo di patologie, accomunate principalmente dalla perdita di funzionalità della catena respiratoria. Come modello di studio di queste patologie abbiamo scelto di utilizzare delle colture primarie di fibroblasti umani derivanti da pazienti con una specifica mutazione nel gene per la subunità ND5 del complesso I della catena respiratoria del DNA mitocondriale. L'utilizzo di questo modello sperimentale si è rivelato molto utile per l'identificazione di una interessante correlazione tra la diminuzione dell'uptake di Ca^{2+} mitocondriale e l'aumento del flusso autofagico in queste cellule. Inoltre, i nostri risultati suggeriscono che la causa del ridotto accumulo di Ca^{2+} mitocondriale è direttamente correlato con un riarrangiamento spaziale nella distribuzione di reticolo endoplasmatico e mitocondri, tale per cui i siti di contatti presenti tra questi due organelli diminuiscono nettamente.

La neurodegenerazione è causata dalla selettiva e progressiva perdita di specifici tipi neuronali. Allo scopo di studiare il coinvolgimento del Ca^{2+} nella neurodegenerazione, abbiamo sviluppato un modello *in vitro* di neuroni primari di corteccia di topo, in cui abbiamo analizzato gli effetti della sovraespressione del canale per il Ca^{2+} mitocondriale, MCU (mitochondrial Ca^{2+} uniporter). Dai nostri dati possiamo concludere che la sovraespressione di MCU ha degli effetti dannosi per le cellule neuronali, tanto da indurne la morte. Inoltre, abbiamo dei risultati preliminari anche in un sistema *in vivo*, i quali confermano e consolidano i dati ottenuti *in vitro*. Nello specifico, abbiamo iniettato vettori adeno-virali esprimenti il canale del Ca^{2+} mitocondriale nel mesencefalo di topo, utilizzando la tecnica dell'iniezione stereotassica, ed anche in questo caso osserviamo l'induzione di morte cellulare e degenerazione neuronale.

INTRODUCTION

Ca^{2+} SIGNALING

General overview

Intracellular signaling requires second messengers, whose concentration rapidly and efficiently varies with time, it follows that one of the most important cellular messengers is Ca^{2+}. Indeed, between cytosol and extracellular environment there are both chemical and electrochemical gradients. Cells invest much of their ATP energy to affect changes in [Ca^{2+}] in space and time (Clapham, 2007).

These rapid modifications in intracellular [Ca^{2+}] require the binding to buffering proteins, the compartmentalization into intracellular stores or the extrusion outside the cell (Berridge, 2009).

Ca^{2+} binding triggers changes in protein shape and charge and consequently activates or inhibits protein functions. The best known protein that buffers Ca^{2+} is calmodulin. This buffering protein and others can control the amplitude and the timing of Ca^{2+} signaling (Hoeflich and Ikura, 2002).

Ca^{2+} signaling in cells consists in dynamic variations of the cytosolic [Ca^{2+}], which at basal level is very low, even small fluctuations are sufficient to induce significant modifications.

Cellular Ca^{2+} fluxes relay on two main sources: the extracellular medium and the internal stores. The most important Ca^{2+} store in the cell is the Endoplasmic Reticulum (ER), but recent works demonstrated that also other organelles, such as Golgi apparatus, endosome and lysosome are able to participate in Ca^{2+} signaling (Pinton et al., 1998) (Calcraft et al., 2009).

The signals that triggers Ca^{2+} changes generate Ca^{2+} waves within the cytoplasm, where it can stimulate numerous physiological Ca^{2+}-sensitive processes, like muscle contraction, hormone secretion, synaptic transmission, cellular proliferation, apoptosis and others (Berridge et al., 2000) (Hajnoczky et al., 1995) (Rizzuto, 2003).

Cells use different types of mechanisms to access to the different Ca^{2+} sourses. These pathways are not exclusive and most cells express combination of them. The best known pathway involves the release of IP3 after stimulation with a hormone, and the consequent release of Ca^{2+} from the ER through the binding to the IP3R.

Once Ca^{2+} has carried out its signaling functions, it is rapidly extruded from the cytoplasm by various pumps and exchangers, and intracellular [Ca^{2+}] returns to resting conditions. The extrusion from the cells or the compartmentalization of Ca^{2+} is due to the action of ATPase pumps, that use ATP like energy sources to maintain low intracellular [Ca^{2+}] by extruding Ca^{2+} from the cells or into intracellular Ca^{2+} stores.

Given that the message decoded by Ca^{2+} is given to the cells like an oscillatory difference of [Ca^{2+}], it is simple to understand the high complexity of pumps and channels that, with their activity, modulate the Ca^{2+} message. During last decades, many scientists focused their attention on the identification of all the import/outport mechanisms for Ca^{2+} signaling, but in spite of this large effort, the whole scenario is not yet completely clear.

Mitochondrial Ca^{2+} signaling

Mitochondria had an important role in the evolution of the eukaryotic cells. These organelles are characterized by a particular structure. They are double membrane-bounded organelles thought to be derived from an proteobacterium-like ancestor, presumably due to a single ancient invasion occurred more than 1.5 billion years ago. The basic evidence of this endosymbiont theory (Dyall et al., 2004) is the existence of the mitochondrial DNA (mtDNA), with structural and functional analogies to bacterial genomes.

Mitochondria are defined by two structurally and functionally different membranes: outer membrane (OMM) and the inner membrane (IMM), characterized by invaginations called “cristae”, which enclose the mitochondrial matrix. The space between these two structures is traditionally called intermembrane space (IMS), but recent advances in electron microscopy techniques shed new light on the complex topology of the inner membrane. Cristae indeed are

not simply random folds, but rather internal compartments are formed by profound invaginations, originating from very tiny "point-like structures" in the inner membrane (Mannella, 2006). These narrow tubular structures, called cristae junctions, can limit the diffusion of molecule from the intra-cristae space towards the IMS, thus creating a micro-environment where respiratory chain complexes, and also other proteins, are hosted and protected from random diffusion.

The OMM contains high copy number of a specific transport protein, VDAC (Voltage-Dependent Anion Channel), which is able to form pores on the membrane, becoming mostly permeable to ions and metabolites up to 5000 Da. However, the IMM is a highly selective membrane, thanks to the presence of cardiolipin, specific phospholipid that make the membrane permeable only to some ions. In addition, on the IMM it is possible to find also other specific transport proteins.

The chemiosmotic theory of energy transfer was first demonstrated by Mitchell (Mitchell, 1967), who showed that the electrochemical gradient across the IMM is utilized by the F1/F0 ATPase to convert the energy of NADH and $FADH_2$, generated by the breaking down of energy rich molecules, such as glucose, into ATP. This gradient is characterized, for the most part, by electrical charge across the membrane ($\Delta\Psi$) and, in minor part it is a H^+ concentration difference between the two compartments (ΔpH). These differences of membrane potential generate a huge driving force that allows the passage of cations through the low sensitive Ca^{2+} channels into the matrix. This gradient is normally maintained in the range of -120/-200 mV.

Mitochondria are very important components of intracellular Ca^{2+} signaling.

Inside mitochondria Ca^{2+} regulates firstly the production of ATP, by the mitochondrial respiratory chain, determining the rate of ATP production (McCormack et al., 1990); in addition, it triggers cellular metabolic adaptation to nutrient levels and it could initiate apoptosis after specific stimuli (Rasola and Bernardi, 2011). Different [Ca^{2+}] in the mitochondrial matrix regulates aerobic metabolism, tuning mitochondrial ATP production in

the needs of a stimulated cell by the control of metabolic enzymes. There are two Kreb cycle's dehydrogenases (isocitrate deidrogenase and α-ketoglutarato deidrogenase) that are Ca^{2+}-sensitive since they directly bind Ca^{2+} and pyruvate dehydrogenase undergoing a dephosphorylating step in a Ca^{2+}-dependent manner (Melendez-Hevia et al., 1996). Thus, the increase in Ca^{2+} level into the matrix modulates the activity of Kreb cycle's enzymes and therefore the passage of electrons through the respiratory chain with the subsequent generation of the gradient across the IMM, which is necessary for ATP production.

When Ca^{2+} has carried out its functions in the mitochondria, it is necessary to rapidly extrude it in order to renew the resting balance into mitochondria. Ca^{2+} extrusion is finely regulated by different exchangers, that are Na+/Ca^{2+} or H+/Ca^{2+} exchangers (Palty et al., 2010).

If this mechanism for the regulation of mitochondrial [Ca^{2+}] fails and high levels of Ca^{2+} are reached in the mitochondria, apoptosis is initiated. These conclusions started from the observation that Bcl-2 has a role in the modulation of Ca^{2+} ions fluxes (Pinton and Rizzuto, 2006).

This protein, like other anti-apoptotic proteins, reduces mitochondrial Ca^{2+} response to extracellular stimuli by reducing the ER Ca^{2+} levels. On the other hand, pro-apoptotic proteins exert their effect by increasing mitochondrial sensitivity. Massive Ca^{2+} entry into mitochondria causes PTP opening that leads to modifications in mitochondrial morphology and the release of pro-apoptotic factors, such as cytochrome c, that initiate the complex cascade of apoptosis.

ER-mitochondria contact sites in Ca^{2+} signaling

A key feature of mitochondria is their spatial organization in the cell. They are not solitary organelles, but they make contact with several other structures, among which the ER has obtained the most attention. Indeed, the physical and functional coupling of these two organelles in living cells, was originally found to determine the transfer of Ca^{2+} between the two organelles.

There are several works in which was underlined the presence of overlapping regions of two organelles (thus establishing an upper limit of 100 nm for their distance) and allowed to estimate the area of the contact sites as 5-20% of total mitochondrial surface (Rizzuto et al., 1993; Rizzuto et al., 1992) (Rizzuto et al., 1998). More recently, electron tomography techniques allowed to estimate an even smaller distance (10-25 nm), as well as the presence of trypsin-sensitive tethers between the two membranes (Csordas et al., 2006).

In mammals, many proteins have been identified to be indirectly involved in the regulation of ER–mitochondria functional interaction, such as some chaperones, PACS-2, BAP31 and NOGO-A.

In the search for the long-sought direct tether, Scorrano and coworkers have recently identified Mfn2 as the first mammalian protein to directly bridge the two organelles. It is retrieved from both ER and mitochondria, and it regulates their morphology. Mfn2 is rich in the ER–mitochondria interface and connects ER with mitochondria via direct interactions between the protein localized in the ER and Mfn1 or Mfn2 present in the OMM.

They also showed that genetic ablation of Mfn2 causes an increase in the distance between the two organelles with a consequent impairment of mitochondrial Ca^{2+} uptake, thus further supporting the high [Ca^{2+}] microdomains theory (de Brito and Scorrano, 2008).

The role of Mfn2 in tethering the two organelles was also confirmed in different systems (Wasilewski et al., 2012) (Area-Gomez et al., 2012).

The mitochondrial Ca^{2+} uniporter (MCU)

During the past, the study of the cellular processes mediated by mitochondrial Ca^{2+} was severely limited by the lack of the molecular identity of the channel responsible of Ca^{2+} entry into the organelle.

A lot of attempts have been made during the decades and several “yet another mitochondrial Ca^{2+} uniporter” have been identified, but without success. Each of them presented critical points that lead these hypothesis to disappear from the scene.

The first important step was obtained from Clapham's group in the 2004, they for first hypothesized and demonstrated the channel's nature of the mitochondrial Ca^{2+} uptake system, that they called MiCa (Kirichok et al., 2004). Nevertheless this important discovery about MCU's nature, the molecular identity of this channel remained unresolved.

The only thinks known for years were the physical properties of the channel, its dependence on mitochondrial membrane potential, its sensitivity to Ruthenium Red and its activity when extramitochondrial [Ca^{2+}] is in the micromolar range.

Subsequently, Graier's group proposed a role of mammalian uncoupling protein (UCP) in the mitochondrial Ca^{2+} uniporter. However, the first results obtained from Trenker et al. have not been confirmed by other groups and also this hypothesis disappeared from the scene (Trenker et al., 2007). In the 2009, Clapham's group tried again to address the issue with a careful genome-wide Drosophila RNA interference (RNAi) screening. The human homolog of CG4589 Letm1 (leucine zipper EF-hand-containing transmembrane protein 1) is an highly conserved homomeric protein that is selectively localized on the inner mitochondrial membrane. In presence of low mitochondrial [Ca^{2+}], it imports Ca^{2+} into mitochondria, representing an important component of the Ca^{2+} entry machinery, but not like so much wanted MCU (Jiang et al., 2009).

Another important study that has allowed to better understand the mitochondrial Ca^{2+} uptake machinery was the discovery of MICU1. Mootha and his collaborators proposed a new and original approach, generating a particular inventory, called MitoCarta and they focused their attention in particular on CBARA1, that they renamed mitochondrial Ca^{2+} uptake 1 (MICU1). They demonstrated that MICU1 is important for mitochondrial Ca^{2+} uptake, but it is composed by only one transmembrane domain. It completely exclude that MICU1 could be a mitochondrial Ca^{2+} uniporter, but only its regulator (Perocchi et al., 2010).

Finally, the 2011 was the lucky year, in which two different groups, independently, identified the "real mitochondrial Ca^{2+} uniporter", they are the our and Mootha's groups. The original

idea was characterized by the in silico investigation. Among the possible 13 candidates, only one was uncharacterized, it was the "coiled-coil domain-containing protein 109A" (ccdc109A). The two groups used different approaches, but the evidences and the conclusions are the same: the long-awaited channel has been discovered (Baughman et al., 2011) (De Stefani et al., 2011). For this reason, hereafter it will be called only MCU.

AUTOPHAGY

The term “autophagy” is derived from the Greek “auto”(self) and “phagy” (eating).

Christian de Duve, who was awarded the Nobel Prize for his work on lysosomes, was the first to use the term autophagy in 1963. He used this word to describe the phenomenon associated with single or double membrane vesicles that contained cytoplasm, including organelles, at various stages of digestion (Deter and De Duve, 1967). Until the early 1990s, autophagy was predominantly studied using morphological and biomedical methods. In the 1992, Ohsumi’s group demonstrated that autophagy occurred in *Saccaromices cerevisiae* and in these organisms was easier study and identify ATG genes (Tsukada and Ohsumi, 1993). The discovery of yeast autophagy genes was followed by the identification of mammalian orthologs with similar roles (Klionsky, 2007). Most ATG genes are well conserved from yeast to mammals.

Have been described three types of autophagic pathways, which differ in their routes to lysosomes: chaperone-mediated autophagy (CMA), microautophagy and macroautophagy.

CMA, unlike the other two processes, involves direct translocation of the targeted proteins across the lysosomal membrane. This direct protein degradation is possible thanks to specific signal sequences called the “KFERQ” motif; in addition, chaperone-mediated autophagy does not involve the degradation of lipids or organelles (Massey et al., 2006).

Microautophagy is the least characterized process, it is used to sequester cytoplasm by invagination and/or septation of the lysosomal/vacuolar membrane (Wang and Klionsky, 2003).

By contrast, the most prevalent form, macroautophagy, involves the formation of cytosolic double membrane vesicles, the autophagosomes, that sequester portions of the cytoplasm (Klionsky and Ohsumi, 1999). Here I will only talk about the macroautophagy, that hereafter I will call only “autophagy.

Autophagy covers several physiological functions, ranging from a basal housekeeping role to response to metabolic stress and regulation of cell death. The relevance of this cellular process at whole organism level is underlined by the observation that the genetic ablation of many ATG genes leads to organism death, due to impaired cell differentiation (Sandoval et al., 2008), embryonic lethality or reduction of survival during peri-neonatal starvation (Kuma et al., 2004).

The repertoire of routine housekeeping functions performed by autophagy includes the elimination of defective or damaged proteins and organelles, the prevention of abnormal protein aggregate accumulation and the removal of intracellular pathogens (Mizushima and Klionsky, 2007). Such functions are critical for autophagy-mediated protection against aging, cancer, neurodegenerative diseases, and infection. Although some of these functions overlap with those of the ubiquitin-proteasome system the other major cellular proteolytic system, but the autophagy pathway is uniquely capable of degrading entire organelles such as mitochondria (in a process called mitophagy), peroxisomes and ER, as well as intact intracellular microorganisms (Kim et al., 2007) (Zhang et al., 2007). Furthermore, the relative role of the autophagy-lysosome system in protein quality control may be greater than it was previously thought.

Moreover, autophagy is activated as an adaptive catabolic process in response to different forms of metabolic stresses, including nutrient deprivation, growth factor depletion and hypoxia. This form of degradation generates free amino and fatty acids that can be recycled to maintain cellular ATP production. Presumably, the amino acids generated are used for the *de novo* synthesis of proteins that are essential for stress adaptation (Levine and Kroemer, 2008).

Autophagy mainly consists in a membrane-trafficking process in which a large number of cytoplasmic components are non-selectively enclosed within a double-membrane structure named autophagosome and delivered to the vacuole-lysosome for degradation and recycling.

The autophagic pathway proceeds through several phases, including: initiation, or formation of pre-autophagosomal structure leading to an isolation membrane, or phagophore; vesicle elongation; autophagosome maturation and cargo sequestration; and autophagosome-lysosome fusion.

In the final step, autophagosomal contents are degraded by lysosomal acid hydrolase and the contents of the auto-lysosome are released for metabolic recycling.

Each step of this process is finely regulated by specific proteins; the fundamental step allowing the correct execution of the autophagic process is the closure of autophagosome. In this step the protein Atg8 and its mammalian ortologues, LC3, GATE16 and GABARAP, play a key role. Atg8/LC3 is an ubiquitin-like protein and it is produced in an inactive form which serves as substrate for the cysteine protease Atg4, which cleaves its substrate thus exposing a glycine residue at its C-terminus. This form of Atg8/LC3, named form I, is unconjugated and soluble and it diffuses throughout the cytosol.

During autophagy, form I Atg8/LC3 becomes phosphatidyletanolamine (PE)-conjugated and membrane-bound, thus producing form II, which is bound to the autophagosome membrane. This process is catalyzed by an ubiquitination-like reaction performed by an E1-like enzyme, Atg7, and an E2-like enzyme, Atg3 (Hanada et al., 2009). Many studies demonstrated that defects in LC3 function or activation lead to the failure of autophagosome closure, thus underlying a central role of Atg8/LC3 in the correct formation of autophagosomes (Fujita et al., 2008) (Sou et al., 2008).

The mammalian target of rapamycin (mTOR) is a primordial negative regulator of autophagy in organisms from yeast to mammalian. mTOR is inhibited under starvation conditions, and this contributes to starvation-induced autophagy via activation of mTOR targets Atg13, ULK1, and ULK2. This inhibition can be mimicked by mTOR inhibitory drugs like rapamycin (Ravikumar et al., 2010).

One of the important pathways regulating mTOR is initiated when growth factors such as insulin-like growth factor bind its receptors (IGF1R). These receptors signal, via their tyrosine kinase activities, activate some effectors like the insulin receptor substrates (IRS1 and IRS2), which in turn activate Akt. Akt inhibits the activity of the TSC1/TSC2 (proteins mutated in tuberous sclerosis) complex, a negative regulator of mTOR. In this way, IGF1R signaling activates mTOR and inhibits autophagy, and the converse occurs when nutrients are depleted.

The TOR kinases are large (about 270kDa) proteins that assemble into two structurally and functionally distinct complexes termed TORC1 and TORC2. In mammalian, TOR (mTOR) associates with raptor to form mTORC1, while it associates with rictor to constitute TORC2. The complex mTORC1 is sensitive to the inhibitory effect of rapamycin: rapamycin, indeed, after forming a complex, can inhibit the proper interaction between mTOR and raptor. This complex is involved in the regulation of cell growth and, under favorable growth conditions, it is active and it promotes ribosome biogenesis and initiation of the translation by inducing the phosphorylation of 4E binding protein 1 (4EBP1) and p70S6K (S6K), which are important to mRNA translation, thus increasing the level of proteins involved in proliferation, cycle progression and survival pathway (Hara et al., 2002).

Moreover, TORC1 acts as a negative regulator of autophagy by sensing environmental change, in particular, it acts as a sensor for a variety of upstream signals, like growth factors, insulin, aminoacids such as leucine and glutamine, intracellular levels of ATP, phosphatidic acid, and inorganic polyphosphates. In mammalian cells, mTOR is regulated by pathway PI3K-Akt, in particular it has been shown that Akt indirectly stimulates TORC1 activity (Sekulic et al., 2000).

TORC2, otherwise, regulates cell growth in a rapamycin-insensitive manner.

Autophagy can also be directly activated by adenosine monophosphate-activated protein kinase (AMPK), which is induced when nutrients are scarce or when ATP/AMP ratios rise, leading to direct Ulk1 activation (Egan et al., 2011) (Kim et al., 2011). In addition, AMPK

could phosphorylate and activate the TSC1/TSC2 complex. The activation of TSC1/TSC2 suppresses mTORC1 activity, inducing autophagy (Matsui et al., 2007) (Wong et al., 2013).

One critical point is that autophagy is a dynamic, multi-step process and so it could be modulated at different steps, both positively and negatively.

For this reason, during the past, it was very complicated understand its progression.

The main important autophagic marker, largely implied for the study of the apoptotic process, is Atg8/LC3 protein, indeed, as I mentioned before, it translocates from cytosol to autophagosomal membranes, following autophagy induction.

In order to monitor the autophagic process, it is possible to use either the endogenous form of the protein or a specific chimera, in which the LC3 protein is fused with a fluorescent protein (usually GFP). This tool allows to visualize the localization of this protein: in resting condition, LC3 is diffused in the cytosol, while upon starvation it shows a punctuate localization, due to its incorporation in the membrane of the forming vesicles.

Given that the autophagosome is an intermediate structure in a dynamic pathway, the number of autophagosomes observed at any specific time point is a function of the balance between the rate of their generation and the rate of their conversion into autolysosomes. Thus, autophagosomes accumulation may represent either autophagy induction or, alternatively, suppression of steps in the autophagy pathway downstream of autophagosome formation.

For this reason, when there is an higher number in autophagosomes, it is not easy distinguish the origin of this increased number. Recently, the literature comes to us suggesting different ways and tools to deeply investigate and study the autophagic process in different systems, in order to distinguish between alteration in autophagic flux or block of it. In our study, we took advantages of these suggestions and indications in order to consolidate our results (Mizushima et al., 2010) (Klionsky et al., 2012).

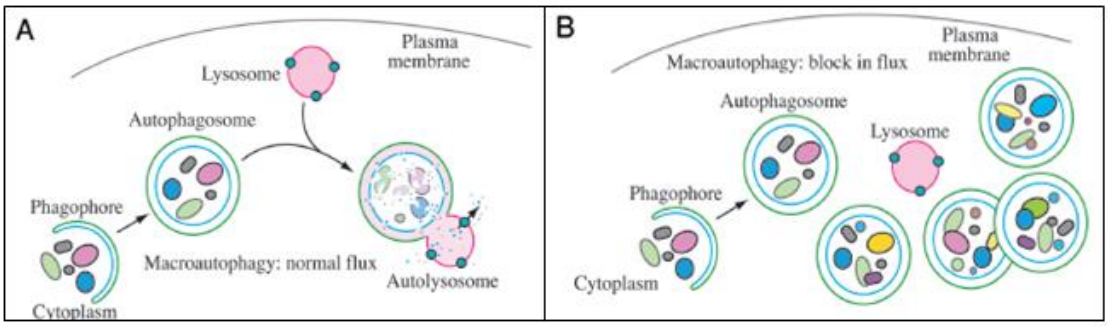

Figure 1.1: Schematic model demonstrating the induction of autophagosomes formation during normal autophagic flux or when turnover is blocked. *(A) The initiation of autophagy includes the formation of the phagophore, the initial sequestering compartment, which expands into an autophagosome. Completion of the autophagosome is followed by fusion with lysosomes and degradation of the contents, allowing compete flux through the entire pathway. (B) There is induction of autophagy, but a defect in autophagosomes turnover, due to a block in fusion with lysosomes or disruption of lysosomal functions, will results in an increased number of autophagosomes (Klionsky et al., 2012) .*

Usually damaged mitochondria are removed by mitophagy, a process where damaged and un-functional mitochondria, that have lost their membrane potential and that are more likely to release toxic apoptotic mediators and reactive oxygen species, are removed via a selective process involving the autophagosome (Pattingre et al., 2005) (Narendra et al., 2008) (Geisler et al., 2010) (Suen et al., 2010). In particular, this mitochondrial elimination could be mediated by the kinase PINK1 and subsequent ubiquitination of mitochondrial membrane proteins by the E3 ligase Parkin (Ravikumar et al., 2010).

Usually the quality control of mitochondrial proteins is ensured by ATP-dependent oligomeric proteases that survey protein quality control within the organelle and aid in the removal of un-assembled and misfolded proteins (Koppen and Langer, 2007). These proteases are found in the mitochondrial matrix, the inner membrane facing the matrix and the inner membrane facing the intermembrane space (Varabyova et al., 2013).

Ca^{2+} dependent control of autophagy

The first report on Ca^{2+}-dependent regulation of autophagy dates back to 1993 (Gordon et al., 1993), and it suggested a complex role for Ca^{2+}, since chelation of either intra- and extracellular Ca^{2+} as well as elevating cytosolic [Ca^{2+}] suppressed autophagy. Only recently this topic returned to be of great interest, many reports describe Ca^{2+} as an inhibitor of autophagy. They are focused, in particular, on the inositol 1,4,5-triphosphate receptor (IP3R), a ubiquitously expressed intracellular Ca^{2+}-releasing channel, located mainly in the ER. IP3Rs mediate Ca^{2+} release from the ER into the cytoplasm in response to different stimuli, like hormones, growth factors or antibodies (Berridge, 2009). In 2005, Sakar et al. reported the use of Li+ for autophagy stimulation (Sarkar et al., 2005). Li+ acts through inhibition of inositol monophosphatase, thereby reducing the IP3 levels. Also chemical inhibition of IP3Rs with xestospongin (XeB) or suppression of its expression using siRNA, also induced autophagy in HeLa cells (Criollo et al., 2007). The IP3R-mediated inhibition of autophagy was also verified in IP3R triple knock out (TKO), which showed higher autophagy levels. In the same work, Cardenas and coworkers showed increased glucose and O_2 consumption, pyruvate dehydrogenase and AMPK activation in TKO cells, suggesting a mechanism whereby constitutive Ca^{2+} release through IP3Rs fuels into the mitochondria, thereby increasing mitochondrial bio-energetics and ATP production (Cardenas et al., 2010). When these essential Ca^{2+} signals are abolished, there is an increased AMP/ATP ratio with a consequent AMPK activation and a subsequent stimulation of autophagy. In this study, the authors cannot exclude a scaffold function for the IP3R.

APOPTOSIS

Apoptosis (also known like “programmed cell death”) is a physiological process used to eliminate damaged, infected or aged cells in multicellular organisms.

Apoptosis is an highly orchestrated process of cell removal necessary for the organism in many physiological situations, such as infections or immune responses.

Differently from necrosis, it is a selective process, that minimizes the tissue damage, eliminating only the damaged cells without immune response.

During apoptosis, it is necessary the ATP consumption and the cellular architecture changes in an highly controlled way, indeed, the apoptotic cells show a series of typical morphological features, like chromatin condensation, cell shrinkage, DNA fragmentation, membrane blebbing. All these events lead to formation of small vesicular bodies, that can be taken up by macrophages.

The apoptotic process is finely regulated, and its negatively or positively dysregulation could lead to some diseases, like neurodegeneration, autoimmunity, viral infections and cancer.

In particular, while uncontrolled proliferation and reduced sensitivity to apoptotic signals are classic hallmarks of oncogenic transformation, excessive and inappropriate apoptosis is the basis of neurodegenerative diseases like Alzheimer.

Molecularly, the execution of the apoptotic program, is due to a family of cysteine proteases called caspases (cysteine aspartic-specific proteases), that cleave substrates at the N-terminal side of a specific aspartic-acid residue. Caspases are synthesized as pro-caspases, which require proteolytical cleavage to form the large and small subunits of the active enzyme. Their activation can happen through autoproteolysis or by other activated caspases.

Apoptosis in mammals can be initiated through two different pathways: the extrinsic pathway involves

extracellular ligands, while the intracellular pathway involves the release of molecules from mitochondria intermembrane space.

In both cases, the apoptotic program is a two-step proteolytical pathway: the first step consists of the activation of “initiator caspases” (caspase 9 and caspase 8), while the second step consists in the activation of “executioner caspases” (caspase 3 and caspase 7), that cleave a number of cellular proteins to drive forward the biochemical events, which culminate in death and dismantling of the cell.

As just said, apoptosis can be triggered through two different pathways. The extrinsic pathway is activated by extracellular molecules binding to the Fas/APO-1 transmembrane protein, which is a member of the tumor necrosis factor receptor (TNFR): when Fas/APO1 binds to its receptor, it induces the recruitment of pro-caspase 8 thanks to the adaptor protein FADD (Fas-associated death domain-containing protein). Upon recruitment to the receptor complex, caspase 8 becomes activated through autoproteolysis and subsequently cleaves and activate caspase-3.

On the other end, in the intrinsic pathway, a central role is played by mitochondria. In particular, the intrinsic pathway is activated by cellular stresses such as DNA damage, heat shock, oxidative stress and many other forms of cellular damage, which result in caspases activation through the release of cytochrome c from mitochondria, following the subsequent bind with Apaf-1 that can oligomerize, thus forming a seven-member ring, the apoptosome, a large caspase activating complex. When it is activated, starts the proteolytical apoptotic cascade.

Interestingly, inside mitochondria cytochrome c is present in two different location: a minor pool is free in inter-membrane space, and a major pool is enclosed in cristae (Delivani and Martin, 2006). The release of cytochrome c, after membrane permeabilization, is performed in two following steps: first the soluble pool and then the pool present in cristae (Scorrano et al., 2002).

The opening of cristae junction plays a key role in apoptosis because in some cell types the soluble cytochrome c is not sufficient to induce the formation of the apoptosome.

The morphology of cristae junction and their opening during apoptosis are regulated by Opa1, a large GTPase also involved in the inner mitochondrial membrane opening (Frezza et al., 2006).

The intrinsic pathway of apoptosis is regulated by members of the Bcl2 family proteins. Bcl2 is the prototype of a large family of proteins, which share a large degree of homology although they exert many different functions, in particular some of them play an anti-apoptotic role, while some other proteins act as pro-apoptotic mediators.

Anti-apoptotic proteins, like Bcl2, BclxL, BclW and Mcl1, have usually four Bcl2 homology (BH) domains, while pro-apoptotic proteins display either three BH domains, like Bax and Bak, or only the BH3 domain, like Bid, Bim and Bad, Noxa and Puma.

It was abundantly demonstrated that these proteins are influenced by $[Ca^{2+}]$, and so it is easy to conclude that the presence of pro-apoptotic or anti-apoptotic proteins, regulated by Ca^{2+} presence, could decide the cellular fate (Pinton and Rizzuto, 2006) (Hajnoczky et al., 2006).

MITOCHONDRIAL DISEASES

At the heart of mitochondria there is the respiratory chain, the core machinery for oxidative phosphorylation. Classically the respiratory chain is defined as a five multi-heteromeric complexes, embedded in the inner mitochondrial membrane. The protein subunits are assembled together and with prosthetic groups and metal containing reactive centers by a set of chaperones, some of them are specific for each complex.

The formation of the respiratory chain is under the control of two different genome: the nuclear (nDNA) and the mitochondrial one (mtDNA). In particular four of the five complexes contain both nuclear-encoded and mitochondrial-encoded polypeptides.

The human mitochondrial genome is a circular, double-stranded molecule composed of 16.6 Kb of DNA, it encodes for 13 protein subunits of the respiratory chain and rRNA and tRNA important for the mitochondrial protein synthesis.

The genetics of mitochondrial DNA differ from the nuclear DNA for some properties: 1) the mitochondrial genome is maternally inherited; 2) mitochondria are polyploidy. Human cells have hundreds of mitochondria, each containing 2-10 mtDNA molecules, at cell division, mitochondria and their genome are randomly distributed to daughter cells; 3) mitochondria lack an efficient repair system, in addition, mitochondrial genome lacks protective proteins like histones and it is physically associated to the inner mitochondrial membrane, where highly mutagenic oxygen radicals are generated as OXPHOS products; 4) normally the mitochondrial genotype of an individual is composed of single mtDNA species, condition known as “homoplasmy”; however, the intrinsic propensity of mtDNA to mutate randomly can occasionally determine a transitory condition known as “heteroplasmy”, where the wild-type and the mutant genome are in the same moment present in the cells. This heteroplasmic condition is a distinctive feature of pathogenic mutations.

Accordingly to the molecular genetic features of the mutation of mtDNA, this group of defects includes clinical syndromes due to large scale rearrangement of the mtDNA; point

mutations of mtDNA and Mendelian traits associated with mtDNA lesions (Zeviani and Antozzi, 1997) (Zeviani and Di Donato, 2004).

In my work, I analyzed only point mutation of mtDNA. Point mutations of mtDNA are usually maternally inherited and can occur in mRNA, tRNA or rRNA genes. Since mtDNA has a very high mutational rate, pathogenic mutations should fulfil the following criteria: high conservation of the affected aminoacids; segregation of the mutation with the clinical phenotype and quantitative correlation between the severity of the clinical and biochemical phenotype and the degree of mtDNA heteroplasmy.

Among the five respiratory chain multi-complexes, the complex I (NADH: ubiquinone oxidoreductase) is the largest and more complicated one, and it forms the major entry point of electrons in the respiratory chain.

Structurally it consists of 45 subunits, 7 encoded by mitochondrial DNA and 38 by nuclear DNA (Carrol et al., 2006). Sequence analysis of the central core demonstrated that it is possible distinguish the 14 subunits in two groups: seven of them are highly hydrophobic, with different number of transmembrane domain and they are encoded by mitochondrial DNA (ND1 to ND6 and ND4L). However, the remaining seven subunits have not any transmembrane domain and they are encoded by nuclear DNA (NDUFV1, NDUFV2, NDUFS1, NDUFS2, NDUFS3, NDUFS7 and NDUFS8) (Brandt, 2006).

In order to facilitate the proper buildup and stability of complex I protein, several assembly chaperones are required (Vogel et al., 2007). The main task of complex I is to take over electrons from NADH to transfer them to ubiquinone, a lipid-soluble carrier of the inner mitochondrial membrane. The energy that originates from this process is used to move protons across the inner membrane, creating an inside negative membrane potential. Importantly, during this process, premature electron leakage to oxygen may occur, this induces an higher superoxide production (Duchen, 2004). Obviously, structural integrity of complex I is essential to maintain the respiratory chain functionality.

In the medical literature the term “mitochondrial disorders” is to a large extent applied to the clinical syndromes associated with abnormalities of the common final pathway of mitochondrial energy metabolism, the oxidative phosphorylation (OXPHOS). Defective oxidative phosphorylation may be due to overall dysfunction of the respiratory chain, or can be associated with single or multiple defects of the five complexes forming the respiratory chain itself.

Given the complexity of mitochondrial genetics and biochemistry, the clinical manifestations of mtDNA disorders are extremely heterogeneous. They range from lesions of single tissues or structures, such as the optic nerve in Leber’s hereditary optic neuropathy (LHON), to more widespread lesions including myopathies, encephalomyopathies, cardiopathies, or complex multisystem syndromes with onset ranging from neonatal to adult life.

Adult patients usually show signs of myopathy associate with variable involvement of the CNS (ataxia, hearing loss, seizures, polyneuropathy, pigmentary retinopathy and, more rarely, movement disorders). Some patients complain only of muscle weakness and/or wasting with exercise intolerance (Zeviani and Carelli, 2003).

In pediatric patients the most frequent clinical features are severe psychomotor delay, generalized hypotonia, lactic acidosis, encephalomyopathies, or isolated myopathies sometimes associated with cardiopathies.

Our experimental model: a MELAS patient with ND5 (13514A>G) mutation

MELAS (*m*itochondrial *e*ncephalomyopathy, *l*actic *a*cidosis, and *s*troke-like episodes) is a multisystem disorder with onset typically in childhood. Early psychomotor development is usually normal, but short stature is common. The onset of symptoms is frequently between two and ten years of age. The most common initial symptoms are generalized tonic-clonic seizures, recurrent headaches, anorexia, and recurrent vomiting. Exercise intolerance or proximal limb weakness can be also initial manifestations. Seizures are often associated with stroke-like episodes of transient hemiparesis or cortical blindness. These stroke-like episodes

may be associated with altered consciousness and may be recurrent. The cumulative residual effects of the stroke-like episodes gradually impair motor abilities, vision, and mentation, often by adolescence or young adulthood. Sensorineural hearing loss is common.

Specifically, in the present work of thesis, we used skin primary fibroblasts derived from a MELAS patient with a novel mtDNA mutation in ND5 subunit of complex I, patient 2 in Corona et al. The 13514A>G mutation caused a D393G change in tis patient, a residue already associated with MELAS phenotype. This patient showed approximately 50% of biochemical activity in both muscle tissue and fibroblasts homogenates.

Clinically, this patient showed the first symptoms of the pathology only at 17 years old, with daily episodes of transitory tingling paresthesias involving her left hand and arm. One year later, permanent visual loss was accompanied by repeated episodes of throbbing headache and transitory prickling paresthesias and weakness of the upper left arm. Contrary to other MELAS cases, this patient did not present lactate acidosis and muscle biopsy was morphologically normal (Corona et al., 2001).

Ca^{2+} SIGNALING in NEURODEGENERATION

Neurons respond to activating stimuli by initiating Ca^{2+} entry through plasma membrane channels, but the consequent increase in free cytosolic Ca^{2+} is strongly modulated by the activity of intracellular Ca^{2+} stores (Clapham, 2007). In particular, Ca^{2+} uptake, sequestration and release by the ER and mitochondria, which are the two major Ca^{2+} regulating organelles, play essential roles in modulating and interpreting Ca^{2+} signals.

Of special interest in this context is a renewed focus on mitochondrial Ca^{2+} handling (Rizzuto and Pozzan, 2006), and the role that this plays in bioenergetics, organelle communication, organelle dynamics and trafficking, cell death signaling, and other equally important aspects of cell signaling. As in other cell types, mitochondria play a pivotal role in neuronal Ca^{2+} signaling (Berridge, 1998).

In addition, mitochondrial Ca^{2+} overload and subsequent dysfunction are thought to be critically important for triggering the cell death that follows ischemic and traumatic brain injury (Friberg and Wieloch, 2002; Norenberg and Rao, 2007; Starkov et al., 2004), as well as in several neurodegenerative disorders including Alzheimer's, Parkinson's, Huntington's and amyotrophic lateral sclerosis (ALS) (Bezprozvanny, 2009; Gibson et al., 2010).

The resting total cellular Ca^{2+} concentration in neurons is typically about 1mM, but the vast majority of intracellular Ca^{2+} is bound to cytosolic proteins or sequestered in the ER. Consequently, baseline free cytosolic Ca^{2+} is usually maintained at 100nM and stimulation could cause global increase to approximately 1μM, local increases may be substantially higher (Meldolesi and Pozzan, 1998; Pozzan and Rizzuto, 2000).

There are large concentration gradients across both plasma membranes and organelle membranes, both at rest and after Ca^{2+} entry and elevation.

Thus, in contrast to the ER, mitochondria do not generally serve as a Ca^{2+} store; however, after stimulation, mitochondria are able to accumulate enormous amounts of Ca^{2+} (Montero et al., 2000; Pivovarova et al., 1999). The accumulation and sequestration of Ca^{2+} within

mitochondria is thought to be profoundly important for processes ranging from synaptic transmission to ischemic brain injury.

Neuronal mitochondria take up Ca^{2+} through the so-called uniporter (De Stefani et al., 2011), a channel that is itself Ca^{2+}-sensitive, and which, when opened by elevated cytosolic Ca^{2+}, allows Ca^{2+} to flow into the matrix down the mitochondrion's steep electrochemical gradient.

Mitochondrial Ca^{2+} release in neurons is regulated primarily by a $Na+/Ca^{2+}$ exchanger. The maximal rate of release is much lower than the maximal rate of uptake, which is why continuous mitochondrial Ca^{2+} accumulation is observed when the cytosolic Ca^{2+} is high. The net effect of the mitochondrial Ca^{2+} transport pathways is that this organelle contains little Ca^{2+} in resting cells, but abruptly begins to accumulate large amounts of Ca^{2+} during stimulated Ca^{2+} entry, and to release this Ca^{2+} load during recovery. This is the typical "buffering" function of mitochondria (Nicholls, 2005).

The physiological effects of elevated intramitochondrial Ca^{2+} are numerous and significant, and include adjusting aerobic ATP production, modulating the effects of elevated cytosolic Ca^{2+} on transmitter release, synaptic transmission and excitability, regulating organelle dynamics and trafficking, mediating signaling to the nucleus, regulating the generation of reactive oxygen species (ROS), and activating the release of death signals. Nonetheless, the mechanisms by which mitochondrial Ca^{2+} accumulation influences global and local Ca^{2+} signals remain incompletely understood, and this continues to be a field of active investigation.

Glutamate is the major excitatory neurotransmitter in the brain. The N-methyl-d-aspartate subtype of the glutamate receptor (NMDAR) plays a central role in excitotoxic injury.

Physiological activation of these receptors permits the flow of cations, primarily Na+ and Ca^{2+}, through their ion channel in a process that is essential for normal synaptic transmission as well as for a variety of Ca^{2+}-dependent signaling pathways. However, massively elevated

levels of glutamate, such as occur in the ischemic core after a stroke, trigger overwhelming NMDAR stimulation, leading to loss of ion homeostasis, cell swelling and necrotic death (Choi and Koh, 1998). In contrast, moderate NMDAR hyperactivity, such as that occurring the ischemic penumbra of a stroke and in many neurodegenerative diseases, results in somewhat less excessive Ca^{2+} influx, which can initiate apoptotic-like damage (Orrenius et al., 2003).

The ability of mitochondria to accumulate enormous amounts of Ca^{2+} in situ plays an important role in excitotoxic injury. There is compelling evidence that excessive Ca^{2+} influx through NMDARs targets mitochondria, leading to mitochondrial Ca^{2+} overload that in turn triggers mitochondrial dysfunction and activation of death signals. However, the precise cellular response to mitochondrial injury is variable, often unclear and controversial. Current models of excitotoxicity implicate one or more of the following mitochondria-related events: uncoupling of oxidative phosphorylation; activation of the mitochondrial permeability transition; release of pro-apoptotic proteins; increased production of ROS and delayed Ca^{2+} de-regulation, ultimately resulting in apoptotic-like cell death. Although the contribution of each of these processes to the activation of death pathways is well established; however, the contribution of other processes, like the direct contribute of the mitochondrial Ca^{2+} uniporter or its regulators is not completely clear.

Neurodegenerative disorders are set of late-onset, progressive, age-dependent brain disorders, characterized clinically by the impairment of cognitive functions, motor coordination, dyskinetic movements, and irreversible changes in behavior and personality. Pathological hallmarks of these disorders including Parkinson's disease (PD), Alzheimer's disease (AD), Huntington's Disease (HD) and Amyotrophic Lateral Sclerosis (ALS), in which there are accumulations of mutant proteins such as α-synuclein, amyloid-β (Aβ), mutant huntingtin (Htt), and super-oxide dismutase (SOD), respectively in the affected brain regions.

Oxidative stress, inflammation, mitochondrial dysfunction, excitotoxicity and impaired transcription have been identified as causal factors for neurodegenerative disorders. Among these, mitochondrial dysfunction takes center stage in the pathophysiology of chronic neurodegenerative disorders. Mitochondria, in general indicate as “power house of the cell” and “ATP reservoir”, are required for the high energy demands of the brain cells including neurons. Any defect of proper functioning of brain mitochondria may lead to severe energy deficiency as well as increased generation of reactive oxygen species (ROS) in neuron and ultimately neuronal demise (Chaturvedi and Flint Beal, 2013).

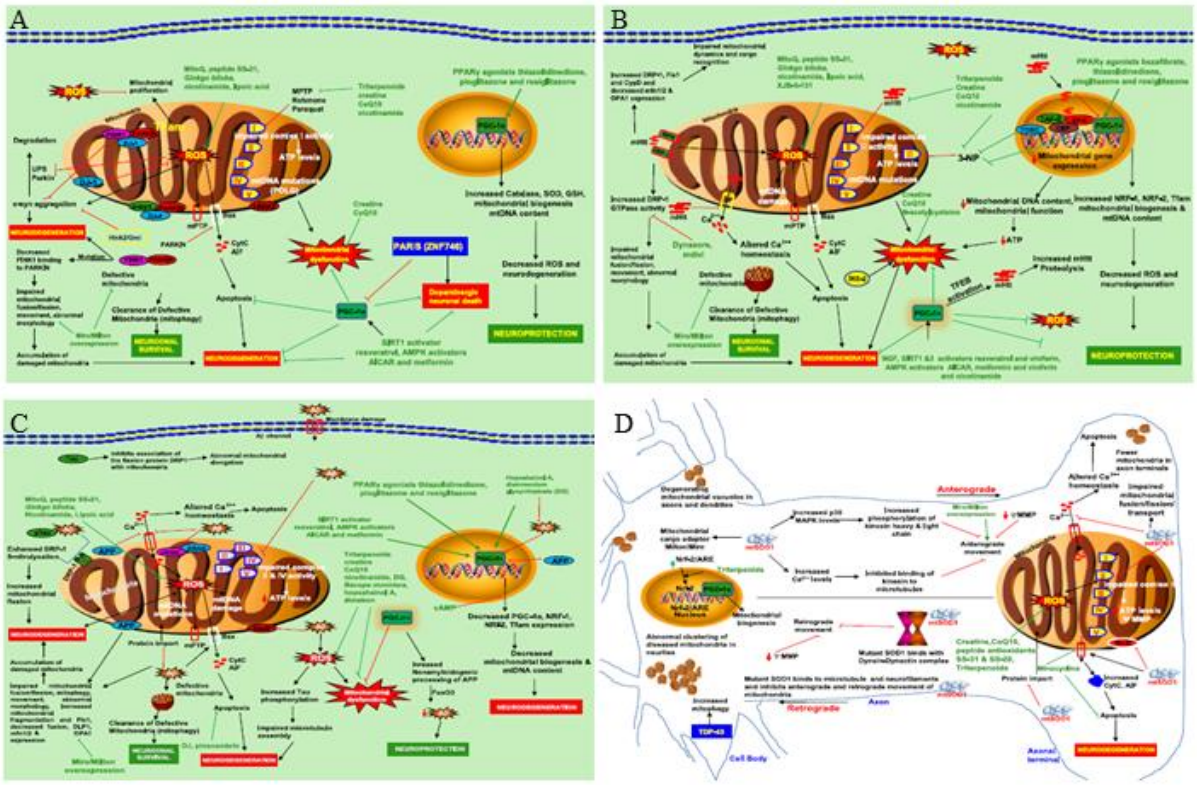

Figure 2: Mitochondrial dysfunction in some neurodegenerative disorders. *Respectively in (A) Parkinson’s disease (PD); (B) Huntington’s disease (HD); (C) Alzheimer’s disease (AD); (D) Amyotrophic lateral sclerosis (ALS) (Chaturvedi and Flint Beal, 2013).*

AIMS

This project was focused on the study of two models of human pathologies, mitochondrial diseases and neurodegeneration: in particular, we investigated the role of mitochondrial Ca^{2+} dynamics in the pathogenesis of these diseases.

Mitochondrial disorders are a large group of heterogeneous diseases that affect organs and tissues with high energy demand, like the brain and skeletal muscle. In our work we wanted to characterize the response to nutrient deprivation (autophagy), Ca^{2+} homeostasis and sensitivity to apoptotic stimuli in cells derived from patients affected by mitochondrial disorders. In particular, we used skin primary fibroblasts derived from patients with complex I ND5 subunit point mutation, as a model for our study.

Secondly, we explored the involvement of mitochondrial Ca^{2+} accumulation in the pathogenesis of neurodegenerative disorders. In order to do that, we used as *in vitro* model of mouse primary cortical neurons and an *in vivo* approach of midbrain stereotaxic injection to overexpress the mitochondrial Ca^{2+} uniporter and thus increase mitochondrial Ca^{2+} uptake to study its role in neurodegeneration.

RESULTS – MITOCHONDRIAL DISEASES

Mitochondria are the primary site for cellular energy production in eukaryotic cells since they host all the enzymes of the respiratory chain (complexes I, II, III, IV and V) and oxidative phosphorylation.

Complex I is the largest multi-subunit complex and is the major entry-point of electrons of the respiratory chain. Mutations in complex I components have serious implications in cell bioenergetics, leading to severe neurodegenerative disorders. Indeed, besides the fundamental function in respiration, mitochondria also have an important role in Ca^{2+} homeostasis, induction of cell death, and autophagy regulation. In line with this, we initially wanted to study the implication of autophagy in mitochondrial diseases, in particular in complex I mutations.

Our experimental model consisted of skin primary fibroblasts, derived from patients with complex I deficiency. This cellular system has several advantages: it allows us to analyze the metabolic properties and the intracellular Ca^{2+} signaling as well as the biochemical and gene expression characterization of patient cells. In addition, it offers the possibility to test and develop new therapeutic approaches to this pathology.

In our experiments, we compared control cells, i.e. fibroblasts from a healthy donor, with fibroblasts from a MELAS (mitochondrial encephalomyopathy, lactic acidosis, and stroke-like episodes) patient with ND5 subunit mutation, harboring the 13514A>G point mutation, changing the D393 residue into a G (D393G) (Corona et al., 2001). Patient characteristics are shown in *Table 1, including* complex I residual activity, the familiarity and the date of birth. Hereafter, cells from this patient are called "Pat" for brief.

Subject	*Date of birth*	*Familiarity*	*Complex I residual activity*	*Affected gene*	*Mutation*	*Hetero plasmy*	*Reference*
Patient	**13-12-1975**	**MELAS**	**60%**	**ND5**	**13514A>G (D393G)**	**25-30%**	**(Corona et al., 2001)**

Table 1: ND5 mutated fibroblasts description.

ND5 mutated fibroblasts show an increased autophagosome number already in basal conditions

Autophagy, from the Greek "auto" (self) "phagy" (to eat), refers to any cellular degradative pathway that involves the delivery of cytoplasmic cargo sequestered inside double-membrane vesicles to the lysosome, in order to generate intracellular nutrients and energy from the degradation of proteins and organelles (Levine and Kroemer, 2008).

Given the emerging role of autophagy as a protective cell response to stress and insults derived from both physiological (such as aging) and pathological (such as in neurodegenerative as well as in mitochondrial disorders) situations, we initially analyzed the cell response to autophagic induction by metabolic stress, which is already existing in complex I mutated fibroblasts.

We then challenged fibroblasts with different protocols of nutrient deprivation, and recorded the induction of autophagy by monitoring specific markers. In particular, we used different models of starvation by changing media composition (DMEM without serum, PBS and KRB saline with or without the addition of glucose) and times (1, 2, 4, 6 hours). We then selected the protocol that gave the more efficient autophagy induction, which is glucose and serum deprivation for 4 hours, hereafter referred to as "starvation condition".

We monitored the appearance of autophagosomes by immunofluorescence, using the membrane-bound lipidated form of LC3 (LC3 II) as a readout. In this way, we were able to count the autophagosome number in control and patient fibroblasts, in basal and starvation conditions.

Our results indicate that there is a clear induction of autophagy activity after starvation conditions in both cell types, and, interestingly, mutated ND5 fibroblasts show higher levels of lipidated LC3 in basal conditions, compared to control, as presented in *Figure 1*.

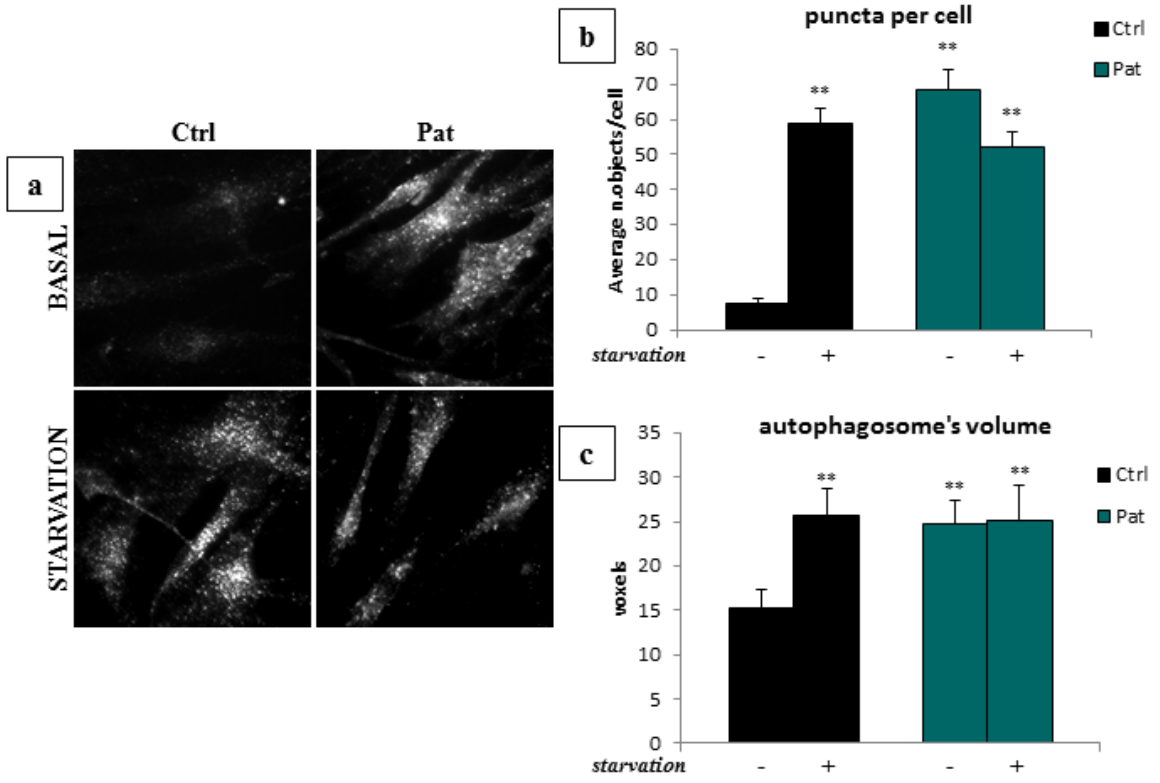

Figure 1: ***<u>ND5 mutated fibroblasts show an increased autophagosome number already in basal conditions.</u>*** *(a) Immunofluorescence analysis with anti LC3-antibody of control (Ctrl) and ND5 mutated fibroblasts (Pat), in basal or starvation conditions. (b) Relative quantification of LC3-positive puncta per cell, of conditions presented in (a)[Ctrl basal:7.4 ± 1.7; Ctrl starvation: 58.9 ± 4.1; Pat basal: 68.6 ± 5.7; Pat starvation: 52.2 ± 4.3]. (c) Relative quantification of autophagosome volume, expressed in voxels, of conditions presented in (a)[Ctrl basal:15.2 ± 2.2; Ctrl starvation: 25.6 ± 3.1; Pat basal: 24.7 ± 2.7; Pat starvation:25.2 ± 3.8].*
Were analyzed at least 200 cells, from 6 different experiments for each condition.
*** P< 0.001.*

<u>The increased autophagosome number in patient cells is not due to a block of the autophagic flux</u>

These first findings opened the question on the cause of the autophagy induction in patient cells; we then wondered if the increase in the autophagosome number is due to an increase in the autophagic flux or rather to a block in the autophagosome degradation pathway.

In order to answer this question, we analyzed the response of control and patient cells to pharmacological inhibition of the final step of autophagy process, which is the fusion of the autophagosomes to lysosomes (Klionsky et al., 2012).

We thus treated our cells with the inhibitor of lysosomal proteolysis, chloroquine, and observed the accumulation of autophagosomes at different time points. Cells with a block in the autophagic flux would have a high autophagosome number already in basal conditions and chloroquine treatment would not affect this. However, our data indicate that chloroquine treatment induces further accumulation of autophagosomes in patients cells, clearly meaning that autophagy induction in ND5 cells is not due to a block of the autophagic flux.

To consolidate these data we looked at another marker of autophagy, the ubiquitin-binding protein sequestosome1, SQSTM1/p62. It is well known its function in the ubiquitination-mediated degradation system, but it is also incorporated into completed autophagosomes and it is degraded in autolysosomes, thus serving as a readout of autophagic degradation (Klionsky et al., 2012).

We evaluated the SQSTM1/p62 protein level by both western blot analysis and immunofluorescence in control and mutated fibroblasts comparing basal and starvation conditions.

We showed that in basal conditions there is a higher protein level of SQSTM1/p62 and also a higher number of SQSTM1/p62 puncta per cell in mutated fibroblasts relatively to control. In addition, no changes after starvation could be appreciated [*Figure 3a, b and c*].

We also evaluated the SQSTM1/p62 mRNA level in order to discriminate if its accumulation in patient cells is due to a transcriptional regulation or to a post-translational mechanism [*Figure 3d*]. The detection of a concomitant increase in the amount of SQSTM1/p62 mRNA and protein level in mutated fibroblasts relative to control cells, demonstrates that the higher number of autophagosomes in mutated fibroblasts, is due to an increase in autophagic flux and not to a block in the degradation pathway.

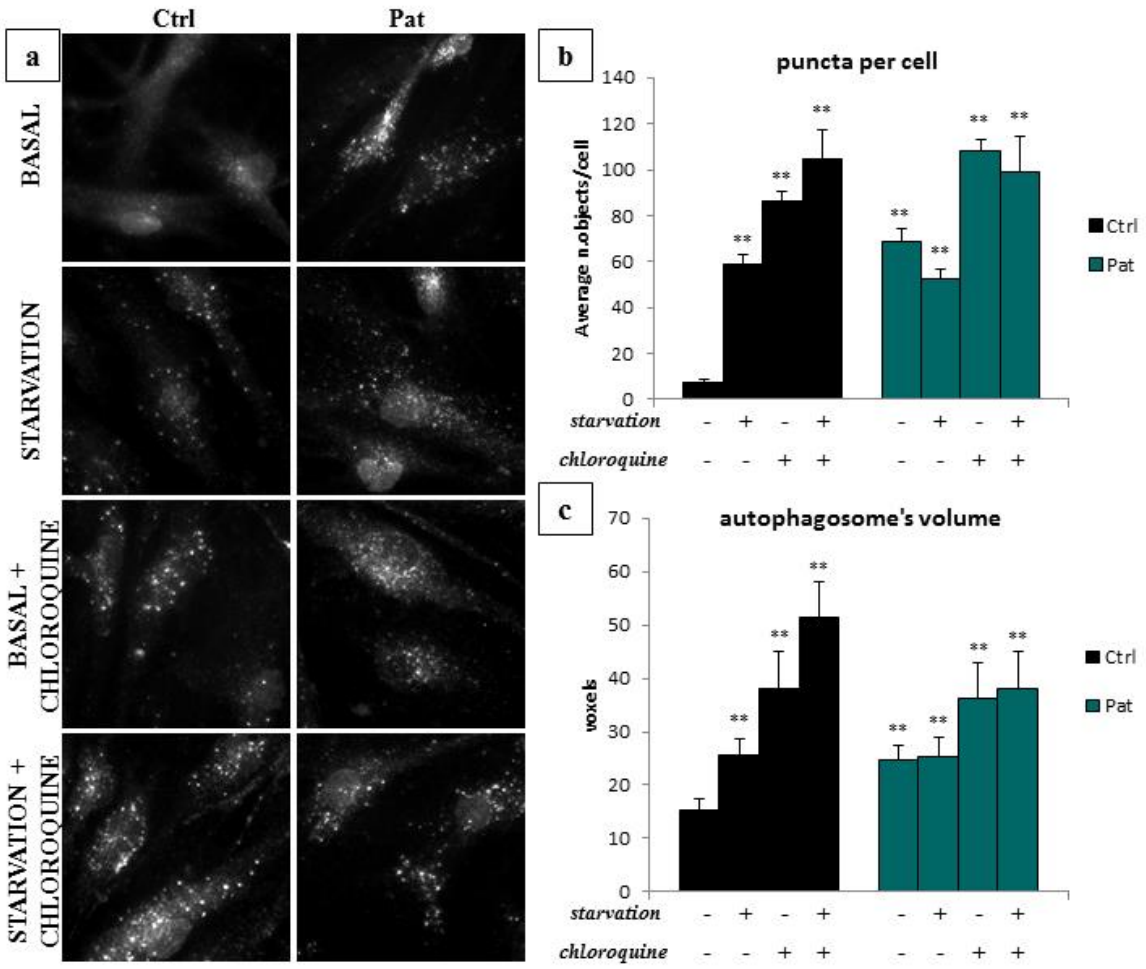

Figure 2: ***<u>The increased autophagosome number in patient cells is not due to a block of the autophagic flux.</u>*** *(a) Immunofluorescence analysis with anti LC3-antibody of control (Ctrl) and ND5 mutated fibroblasts (Pat), in basal or starvation conditions and with or without chloroquine treatment (50 μM for 1 hour). (b) Relative quantification of LC3-positive puncta per cell, of conditions presented in (a) [Ctrl basal:7.4 ± 1.7; Ctrl starvation: 58.9 ± 4.1; Ctrl basal+chloroquine: 86.4 ± 4.2; Ctrl starvation+chloroquine: 104.5 ± 12.9; Pat basal: 68.6 ± 5.7; Pat starvation: 52.2 ± 4.3; Pat basal+chloroquine: 108.5 ± 4.8; Pat starvation+chloroquine: 99.1 ± 15.7]. (c) Relative quantification of autophagosome volume, expressed in voxels, of conditions presented in (a)[Ctrl basal:15.2 ± 2.2; Ctrl starvation: 25.6 ± 3.1; Ctrl basal+chloroquine: 38.0 ± 7.1; Ctrl starvation+chloroquine: 51.3 ± 6.9; Pat basal: 24.7 ± 2.7; Pat starvation:25.2 ± 3.8; Pat basal + chloroquine: 36.2 ± 6.6; Pat starvation+chloroquine: 37.9 ± 6.9]. Were analyzed at least 150 cells, from 4 different experiments for each condition.** P< 0.001.*

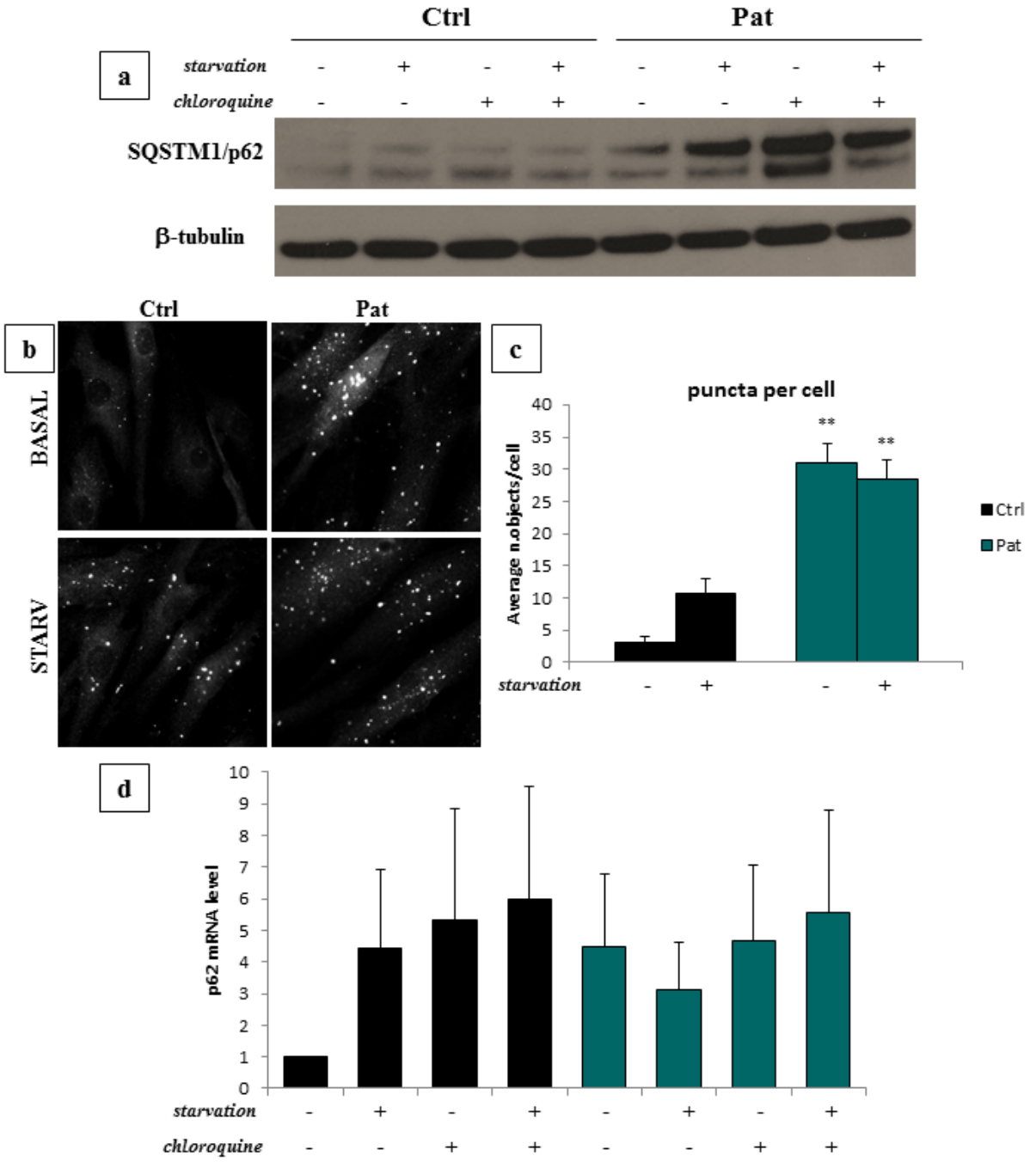

Figure 3: ***<u>The autophagy related SQSTM1/p62 accumulates in patient cells already in basal conditions.</u>*** *(a) Immunoblot analysis of SQSTM1/p62 and β-tubulin proteins of control (Ctrl) and ND5 mutated fibroblasts (Pat). (b) Immunofluorescence analysis with anti SQSTM1/p62-antibody of control (Ctrl) and ND5 mutated fibroblasts (Pat), in basal or starvation conditions. (c) Relative quantification of SQSTM1/p62-positive puncta per cell, of conditions presented in (b)[Ctrl basal:3.1 ± 1.0; Ctrl starvation: 10.6 ± 2.4; Pat basal: 31.0 ± 3.0; Pat starvation: 28.5 ± 3.0]. (d) SQSTM1/p62 mRNA level, normalized to Rpl32 mRNA level, of control (Ctrl) and ND5 mutated fibroblasts (Pat), in basal and starvation conditions [Ctrl basal:1; Ctrl starvation: 4.43 ± 2.5; Ctrl basal+chloroquine: 5.32 ± 3.5; Ctrl starvation+chloroquine: 5.99 ± 3.6; Pat basal: 4.46 ± 2.3; Pat starvation: 3.14 ± 1.5; Pat basal+chloroquine: 4.68 ± 2.4; Pat starvation+chloroquine: 5.55 ± 3.2].*
*The measurements were performed form 3 different experiments. ** P< 0.001.*

Mitochondria are direct substrates of autophagy in patient fibroblasts

We next investigated whether mitochondria of complex I mutated cells could be possible substrates of autophagy.

To answer this, we then monitored protein level of two mitochondrial markers by western blot, Tom20 (the outer mitochondrial membrane translocase protein), and Hsp60 (a mitochondrial matrix protein), in control and mutated fibroblasts, comparing basal and starvation conditions. These two proteins do not show any changes in their levels despite the different cell genotypes or treatments applied [*Figure 4a*].

Although removal of damaged or dysfunctional mitochondria through mitophagy could be one mechanism by which the mitochondrial pool in mutated fibroblasts is maintained, these data suggest that mitophagy is not up-regulated in these cells.

We decided to further investigate this by testing the response of control and mutated fibroblasts to treatments that selectively induce mitophagy. We used the mitochondrial uncoupler carbonyl m-chlorophenyl hydrazine (CCCP) to induce mild mitochondrial damage, and we subsequently monitored the removal of damaged organelles over time, by examining the protein levels of mitochondrial markers. We showed that the process of mitochondrial removal is significantly accelerated in mutated fibroblasts. Indeed, all the mitochondrial markers analyzed disappear faster in mutated than control fibroblasts [*Figure 4b*], indicating that mitochondria are substrates of the increased autophagic flux in ND5 fibroblasts.

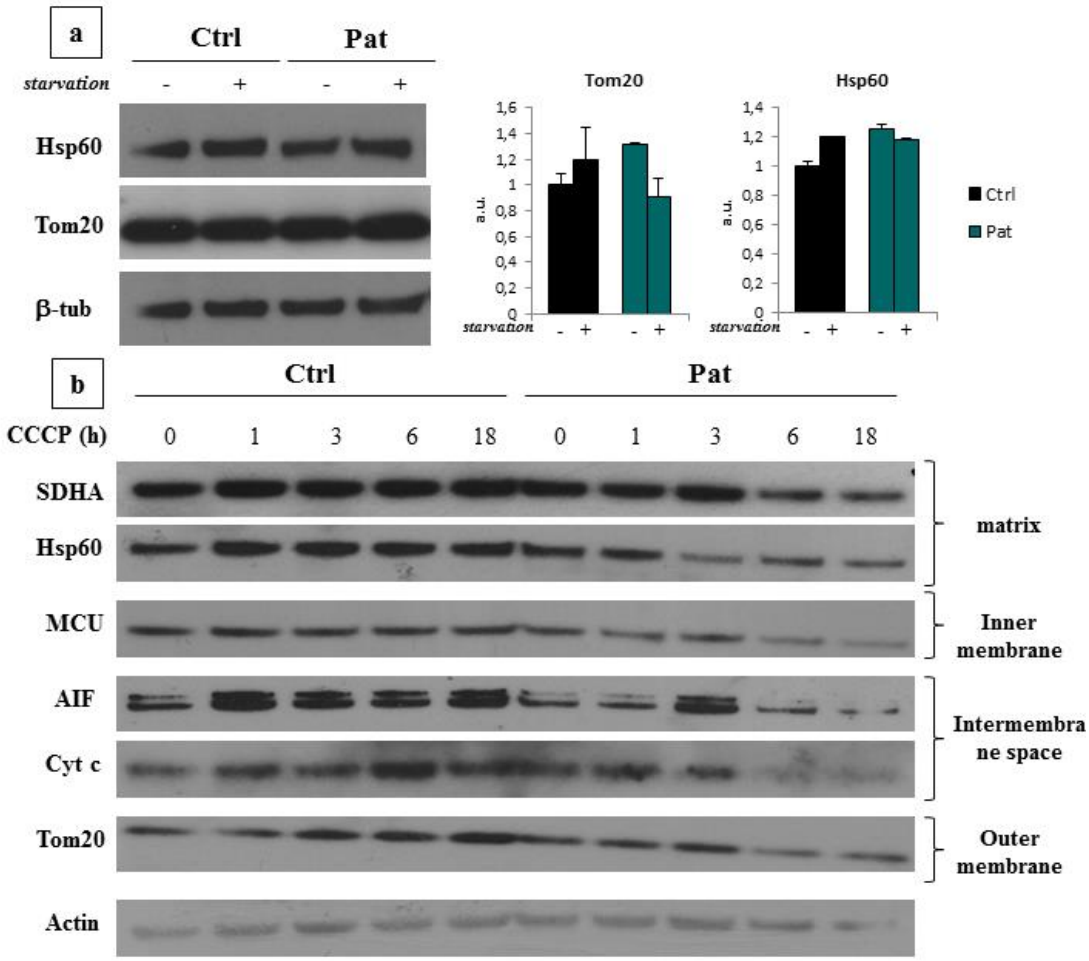

Figure 4: ***<u>Mitochondria are direct substrates of autophagy in patient fibroblasts.</u>*** *(a) Immunoblot analysis of Hsp60, Tom20 and β-tubulin proteins of control (Ctrl) and ND5 mutated fibroblasts (Pat), with the relative quantification of Hsp60 and Tom20 levels. β-tubulin was used as loading control. (b) Immunoblot analysis of SDHA, Hsp60, MCU, AIF, Cyt c, Tom20 and Actin proteins of control (Ctrl) and ND5 mutated fibroblasts (Pat), after 0 – 1 – 3 – 6 – 18 hours of CCCP treatment (10μM), respectively.*
The blots are representative of 3 different experiments.

<u>ND5 mutated fibroblasts show an alteration selectively in mitochondrial Ca^{2+} homeostasis</u>

Recently, Cardenas et al. reported that constitutive low level of IP3R-mediated Ca^{2+} release has an important role in the maintenance of optimal cellular bioenergetics and autophagy (Cardenas et al., 2010), and keeping in mind these information, we decided to investigate the role of Ca^{2+} homeostasis in our model of mitochondrial disorders.

We took advantage of the established expertise of our laboratory in the measurements of Ca^{2+} dynamics in different cell compartments, and we utilized the bioluminescent protein probe aequorin to calculate the sub-cellular Ca^{2+} concentration in the cytosol, ER and mitochondria of control and ND5 mutated fibroblasts, after IP3-mediated agonist stimulation (Granatiero et al., 2014; Pinton et al., 2007).

Our results point out that ND5 mutated cells do not present any alteration of Ca^{2+} dynamics in the cytosol and ER [*Figure 5a* and *b*]; however, they clearly show a significant decrease in Ca^{2+} uptake selectively in mitochondria, as demonstrated by experiments performed in both intact and permeabilized cells [*Figure 5c* and *d*].

ND5 mutated fibroblasts are protected from apoptosis

This observed decrease in mitochondrial Ca^{2+} uptake in fibroblasts with complex I mutation suggested the possibility that these cells could be also protected from apoptosis, given the widely accepted crucial role of mitochondrial Ca^{2+} load in the trigger of apoptosis (Orrenius and Nicotera, 1994).

We decided to challenge our cells with Staurosporine, a well-known apoptotic stimulus (Caballero-Benitez and Moran, 2003), and we monitored the conversion of Caspase3 into its active, cleaved form by immunofluorescence, in order to understand the sensitivity to apoptosis of our cells.

As expected, we observed a higher resistance to staurosporine treatment in ND5 mutant cells [*Figure 6*].

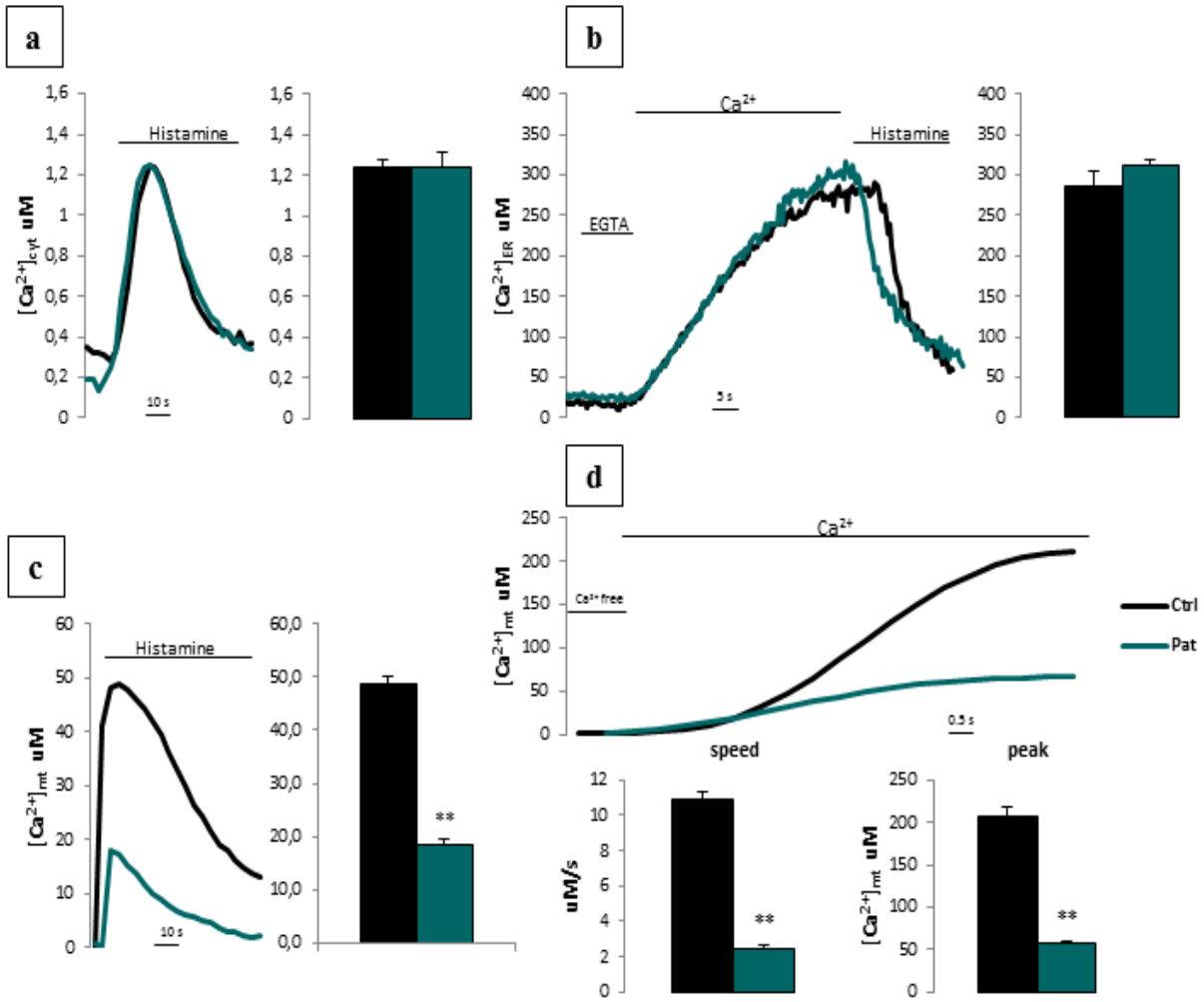

Figure 5: ***<u>ND5 mutated fibroblasts show an alteration selectively in mitochondrial Ca^{2+} homeostasis.</u>*** *(a) Representative traces of cytosolic Ca^{2+} level after agonist stimulation (histamine 100μM), of control (Ctrl) and ND5 mutated fibroblasts (Pat), with the relative quantification of cytosolic Ca^{2+} peak: 1.2 ± 0.04 μM and 1.2 ± 0.07 μM, respectively. (b) Representative traces of ER Ca^{2+} uptake and release, after addition of $CaCl_2$ 1mM and histamine 100μM, for other details see Materials and Methods), of control (Ctrl) and ND5 mutated fibroblasts (Pat), with the relative quantification of ER Ca^{2+} content: 285.7 ± 19.3 μM and 311.7 ± 7.7 μM, respectively. (c) Representative traces of mitochondrial Ca^{2+} uptake in intact cells, after agonist stimulation (histamine 100μM), of control (Ctrl) and ND5 mutated fibroblasts (Pat), with the relative quantification of mitochondrial Ca^{2+} peak: 39.6 ± 2.7 μM and 16.36 ± 1.2 μM, respectively. (d) Representative traces of mitochondrial Ca^{2+} uptake in permeabilized cells, after addition of $CaCl_2$ 2mM, of control (Ctrl) and ND5 mutated fibroblasts (Pat), with the relative quantification of the Ca^{2+} peaks: 208.1 ± 9.3 μM and 57.1 ± 1.8 μM, respectively, and speed of uptake: 10.9 ±0.5 μM/s and 2.5 ± 0.1 μM/s, respectively. All the Ca^{2+} measurements are performed using aequorin probe specifically targeted to different compartments (for more details see Material and Methods). The measurements were performed at least for 30 samples from 6 different experiments. ** P< 0.001.*

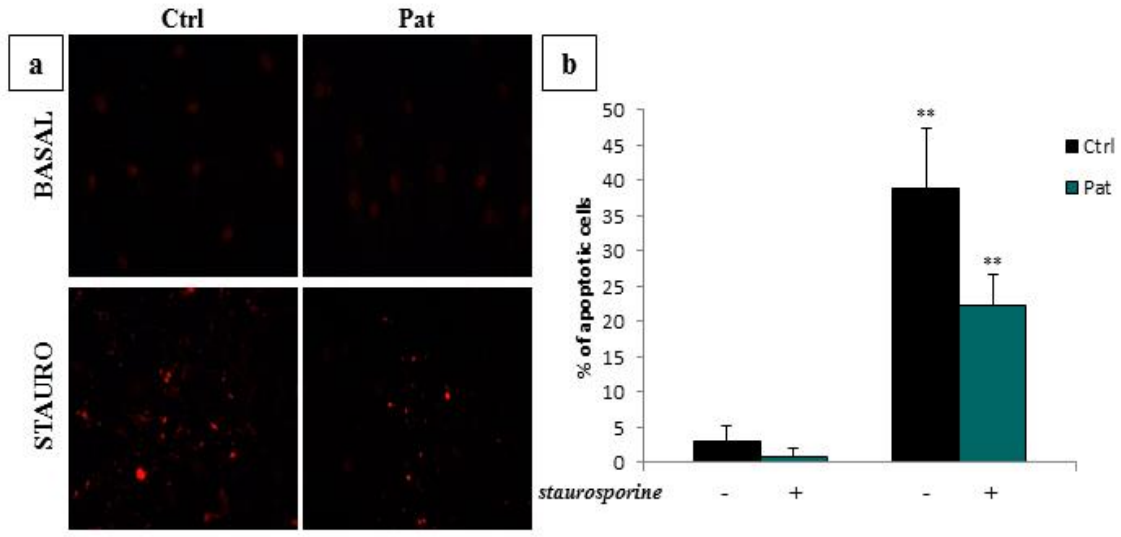

Figure 6: ***<u>ND5 mutated fibroblasts are protected from apoptosis.</u>*** *Immunofluorescence analysis with anti cleaved Caspase3-antibody of control (Ctrl) and ND5 mutated fibroblasts (Pat), with or without staurosporine treatment (500nM for 16 hours), with relative quantification of the percentage of cleaved Caspace3-positive or apoptotic cells [Ctrl basal: 3.1 ± 2.1; Ctrl staurosporine: 39.0 ± 8.3; Pat basal: 1.0 ± 1.1; Pat staurosporine: 22.3 ± 4.5]. Were analyzed 60 random fields for each condition, from 3 different experiments.*
*** P< 0.001.*

<u>Patient cells do not present alterations in mitochondrial morphology and membrane potential, but show a clear deficiency in ER-mitochondria contact sites</u>

In order to understand the origin of the observed decrease in mitochondrial Ca^{2+} uptake in patient cells, we decided to analyze different mitochondrial parameters, starting from the mitochondrial membrane potential.

We performed experiments using the Rhodamine-derived lipophilic dye TMRM (Tetra-Methyl-Rhodamine-Methyl Ester) to monitor mitochondrial membrane potential over time and after treatments with ATP synthase inhibitor oligomycin or the complex I blocker rotenone, to challenge cells to maintain the membrane potential by ATP hydrolysis through the reverse activity of complex V. We observed no differences between conditions.

As you can see from *Figure 7a*, after rotenone treatment the mitochondrial membrane potential is maintained by ATP hydrolysis as is shown by addition of oligomicyn, and there is no difference between ND5 mutant and control cells. We performed also the reverse experiment using oligomycin first and then rotenone, and we obtained same results (data not shown). This means that these cells are able to maintain the mitochondrial membrane potential, probably due to up-regulation of other respiratory chain complexes.

This is in line with our mitochondrial morphology data, showing no alteration in mitochondrial network size and distribution in ND5 cells compared to control [*Figure 7b*].

We next wanted to explore the molecular factors and complexes mediating the Ca^{2+} entry in the organelle. Since the 60s, the existence of a mitochondrial Ca^{2+} uniporter (MCU) was described (Deluca and Engstrom, 1961), but the molecular identification was finally revealed only in 2011 by the work of our group (De Stefani et al., 2011) and another (Baughman et al., 2011).

To investigate this, we performed western blot analysis of the protein level of MCU in control and ND5 mutated cells and no differences were found [*Figure 7c*].

We also analyzed the levels of the major regulators of MCU: MICU1 and MICU2 (Mallilankaraman et al., 2012; Patron, 2014; Perocchi et al., 2010), which show little but significant alterations in mutated fibroblasts relatively to control cells [*Figure 7d*]. However, these alterations cannot explain the decrease in mitochondrial Ca^{2+} uptake observed in complex I deficient cells, as elegantly demonstrated in Patron et al. (Patron, 2014). It appears that the content of MCU and related proteins is not a factor in mutated cells.

The rapid accumulation of mitochondrial Ca^{2+}, besides to the electrochemical gradient driving force generated by the respiratory chain activity, depends on the strategic location of mitochondria and the establishment of close contact sites with the ER, which is the main cellular Ca^{2+} store (Rizzuto et al., 1998; Rizzuto and Pozzan, 2006).

For the fine localization and interaction of cellular components, we took advantage of the described research tool based on split GFP technology (Cabantous et al., 2005), utilizing the specific version of this split GFP system, engineered by Dr. Tito Calì (unpublished data), to explore the abundance and the distribution of these mitochondria-ER contact sites in our cellular model.

In this system the GFP is divided in two parts, the first one is directly bound to an outer mitochondrial membrane protein, while the last GFP strand is directly bound to an ER protein. The transfection of this probe allows the detection of the green fluorescence only when the two parts of GFP are close enough to reconstitute the fluorescent protein, in this way we were able to detect the contact sites between ER and mitochondria as green fluorescent dots and count them, by specific ImageJ analysis software.

When transfected in control and ND5 mutated cells, this split GFP probe showed a significantly reduced number of contact sites in mutated cells compared to control [*Figure 7e*].

Accordingly, the expression level of Mitofusin 2 (MFN2), one of the proteins present in specialized regions of mitochondria-ER contacts, is also reduced in patients cells [*Figure 7f*].

Together these results clearly indicates that the reason of the decrease in mitochondrial Ca^{2+} uptake in mutated cells is the presence of fewer contact sites between ER and mitochondria.

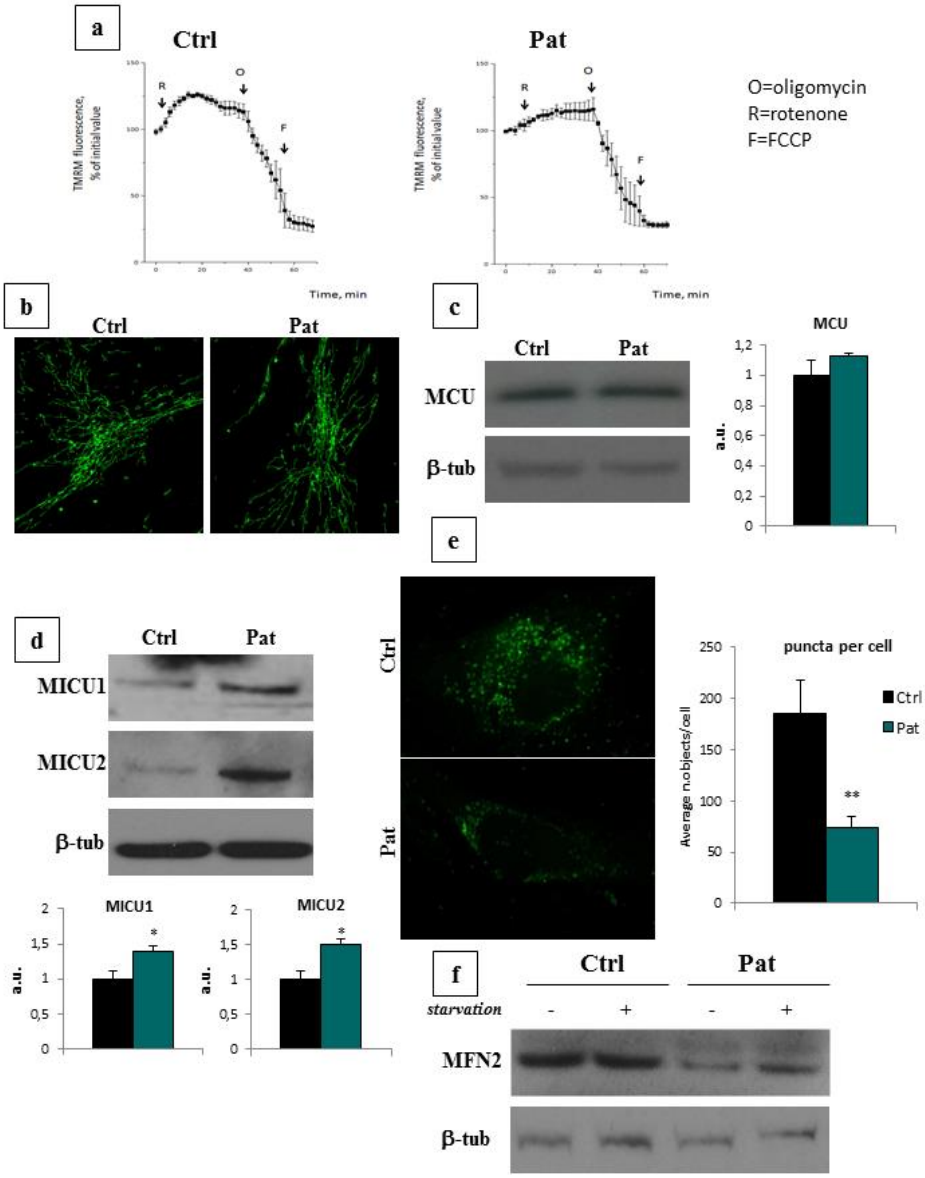

Figure 7: ***<u>Patient cells do not present alteration in mitochondrial morphology and membrane potential, but show a clear deficiency in ER-mitochondria contact sites.</u>*** *(a) Measure of the mitochondrial membrane potential by TMRM probe (20nM for 30 minutes of incubation), of control (Ctrl) and ND5 mutated fibroblasts (Pat), after rotenone (4μM), oligomycin (5μM) and FCCP (4μM) addition. (b) Immunofluorescence analysis with anti Tom20-antibody of control (Ctrl) and ND5 mutated fibroblasts (Pat). (c) Immunoblot analysis of MCU and β-tubulin proteins of control (Ctrl) and ND5 mutated fibroblasts (Pat), with the relative quantification of MCU levels. β-tubulin was used as loading control. (d) Immunoblot analysis of MICU1, MICU2 and β-tubulin proteins of control (Ctrl) and ND5 mutated fibroblasts (Pat), with the relative quantification of MICU1 and MICU2 levels. β-tubulin was used as loading control. (e) Detection of contact sites between ER and mitochondria, using specific split GFP (for more details see Materials and Methods) in control (Ctrl) and ND5 mutated fibroblasts (Pat), with the relative quantification: 184.9 ± 33.1 and 73.5 ± 11.8, respectively. (f) Immunoblot analysis of MFN2 and β-tubulin proteins of control (Ctrl) and ND5 mutated fibroblasts (Pat), with the relative quantification of MFN2 bands. β-tubulin was used as loading control. The measurements were performed form 3 different experiments. ** P< 0.001.*

MCU overexpression induces a reduction in autophagosome number in patient fibroblasts

Our results suggest an interesting scenario for our mitochondrial disorder model, which appears to be characterized by increased autophagic flux and decreased mitochondrial Ca^{2+} uptake.

At this point, we wanted to study in more detail the correlation between these two features and in particular to explore the possibility of modulating the induction of autophagic flux by influencing the mitochondrial Ca^{2+} homeostasis.

In order to do this, we overexpressed MCU in control and complex I deficient fibroblasts. As expected, MCU overexpression raised the mitochondrial Ca^{2+} uptake in control cells and, more interestingly, was able to restore the level of mitochondrial Ca^{2+} of ND5 patient fibroblasts to control [*Figure 8a*].

We then measured the formation of autophagosomes in MCU overexpressing cells, with the same approach previously described. As presented in *Figure 8b*, MCU overexpression and the consequent increase in mitochondrial Ca^{2+} uptake, caused a significant reduction of the abnormally high number of autophagosomes present in ND5 cells in basal conditions. This suggests a direct correlation between increased mitochondrial Ca^{2+} accumulation and autophagy suppression.

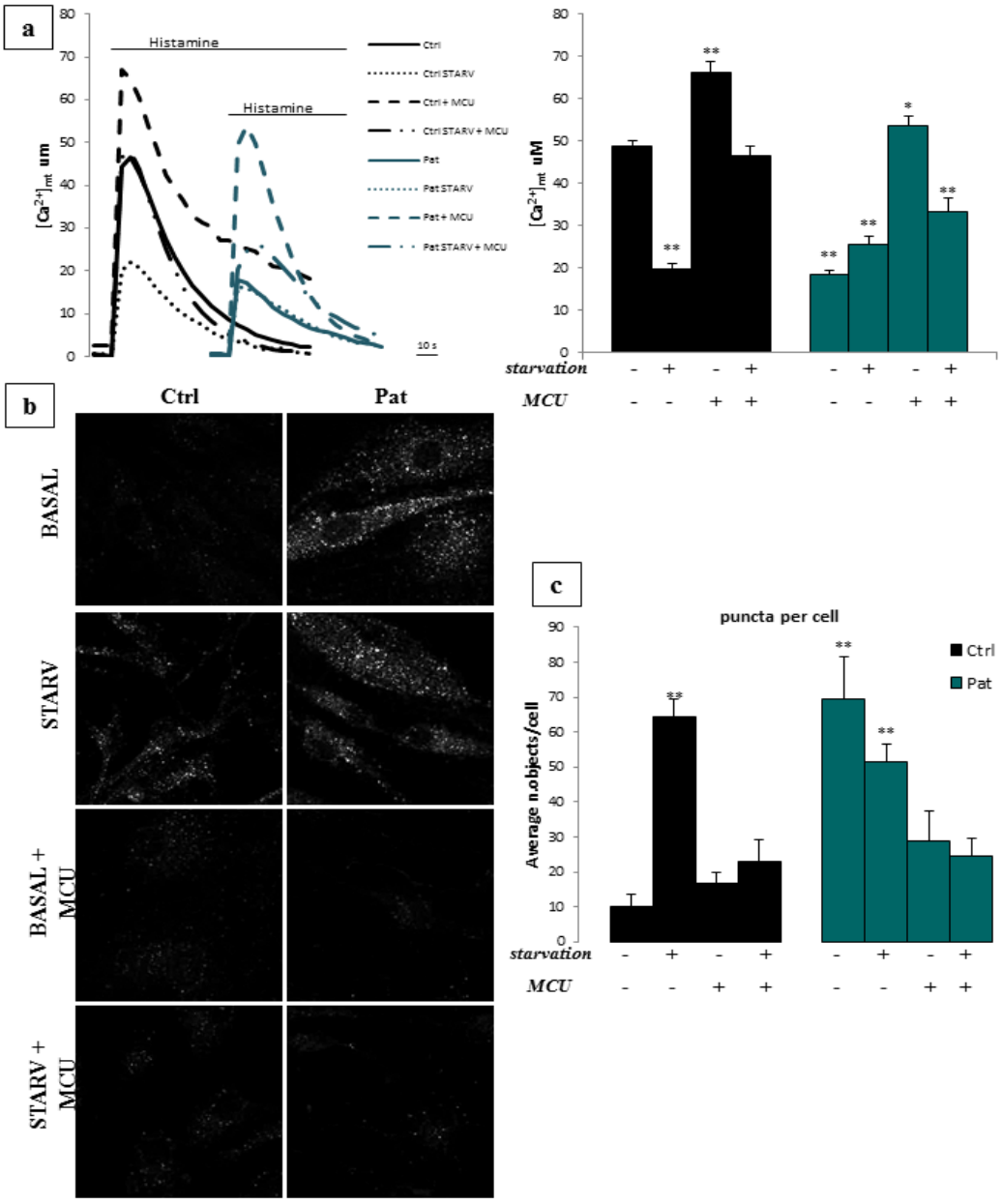

Figure 8: <u>MCU overexpression induces an increase in mitochondrial Ca^{2+} uptake and a reduction of autophagosome number in patient fibroblasts.</u> *(a) Representative traces of mitochondrial Ca^{2+} uptake in intact cells, after agonist stimulation (histamine 100 μM), of control (Ctrl) and ND5 mutated fibroblasts (Pat), in basal and starvation conditions, with or without the MCU overexpression, with the relative quantification of mitochondrial Ca^{2+} peak [Ctrl basal: 48.7 ± 1.5 μM; Ctrl starvation: 19.7 ± 1.3 μM; Ctrl basal+MCU: 66.2 ± 2.5; Ctrl starvation+MCU: 46.4 ± 2.1 μM; Pat basal:18.4 ± 1.1 μM; Pat starvation:25.6 ± 2.0 μM; Pat basal+MCU: 53.5 ± 2.3 μM; Pat starvation+MCU: 33.5 ± 3.2 μM]. The measurements were performed at least for 25 samples from 5 different experiments. (b) Immunofluorescence analysis with anti LC3-antibody of control (Ctrl) and ND5 mutated fibroblasts (Pat), in basal or starvation conditions and with or without MCU overexpression. (c) Relative quantification of LC3-positive puncta per cell, of conditions presented in (b)[Ctrl basal:7.4 ± 1.7; Ctrl starvation: 58.9 ± 4.1; Ctrl basal+MCU: 16.9 ± 2.9; Ctrl starvation+MCU: 24.7 ± 5.2; Pat basal: 68.6 ± 5.7; Pat starvation: 52.2 ± 4.3; Pat basal+MCU: 27.7 ± 3.7; Pat starvation+MCU: 25.6 ± 2.5]. Were analyzed at least 100 cells, from 3 different experiments for each condition.** P< 0.001.*

The AMPK pathway is involved in the regulation of autophagic flux in mutated fibroblasts

In order to understand which are the molecular pathways implicated in the link between the control of autophagy and the level of mitochondrial Ca^{2+}, we analyzed some of the main signaling factors involved in the autophagy machinery.

We measured Akt phosphorylation level by western blot, in particular the Ser473 residue which is well known to be involved in the activation of autophagy (Bayascas and Alessi, 2005). However, we did not see any difference between control and mutated fibroblasts [*Figure 9a*]. We also looked at the mammalian target of rapamycin (mTOR), specifically mTORC1, the central player in the regulation of autophagy, and its downstream effector S6 protein (Alers et al., 2012; Jung et al., 2010). Also in this case, the western blot analysis did not reveal any significant differences in mTOR or S6 phosphorylation between mutated and control cells [*Figure 9a*].

Another important mediator of the response to metabolic stresses associated with nutrient availability is the AMP-activated protein kinase (AMPK), which is a critical metabolic sensor of AMP/ATP ratio (Hardie, 2007) and, as already mentioned, has been shown to be involved in the stimulation of autophagy in response to altered ER Ca^{2+} release (Cardenas et al., 2010).

We thus measured AMPK phosphorylation by western blot, in particular at Ser 172, which is a mTOR-independent phosphorylation site (Andersen and Rasmussen, 2012). We were able to detect a significant difference in AMPK between control and mutated fibroblasts, namely AMPK phosphorylation is greatly induced in mutated fibroblasts [*Figure 9b*].

The implication of the AMPK pathway in this scenario is also supported by its increased phosphorylation in cells overexpressing MCU. Indeed, as shown in *Figure 9c*, MCU overexpression in ND5 patients fibroblasts, besides modulating the autophagic flux, also decreases AMPK phosphorylation, restoring it to the level of control cells.

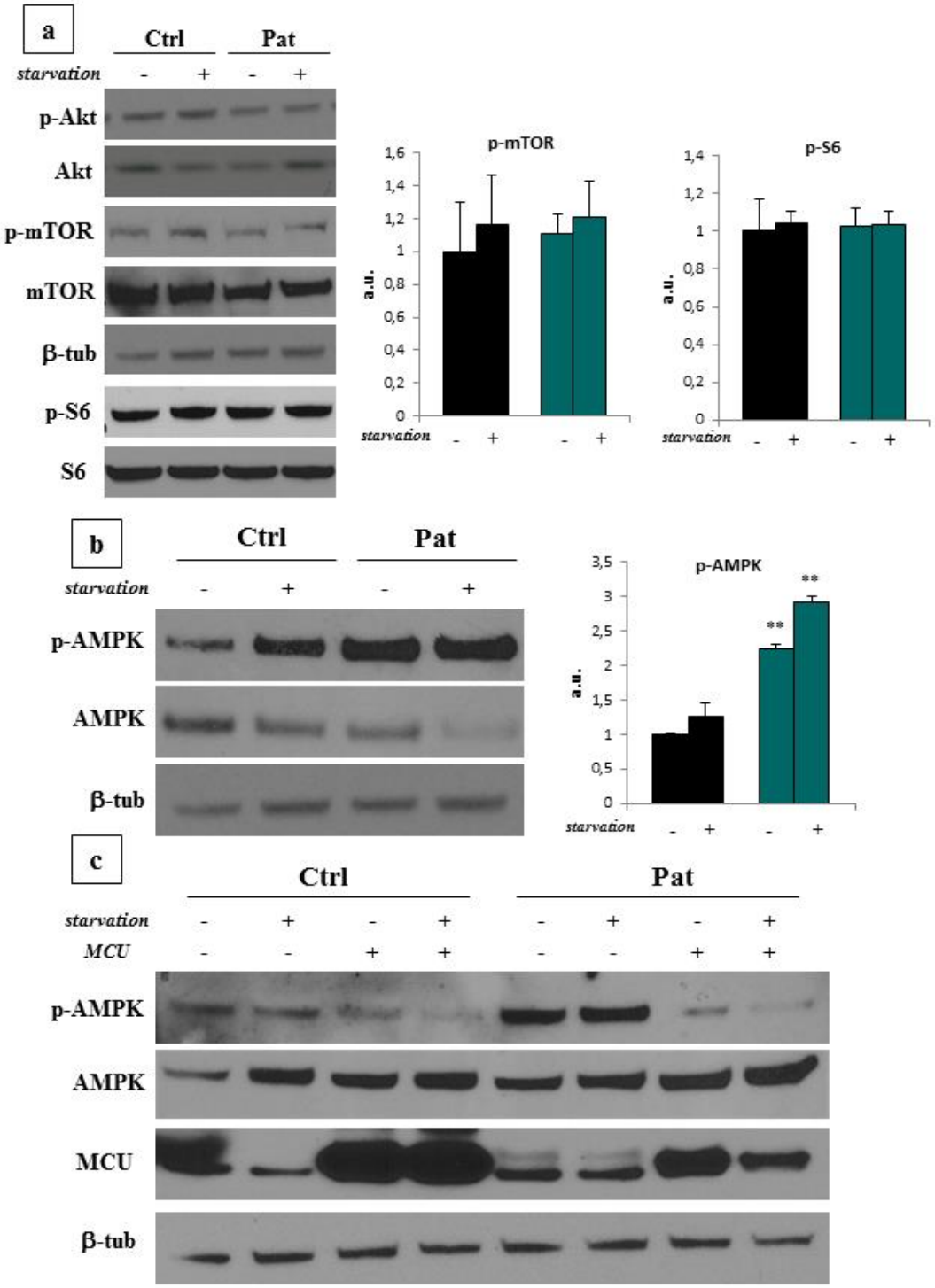

Figure 9: ***<u>The AMPK pathway is involved in the regulation of autophagic flux in mutated fibroblasts.</u>*** *(a) Immunoblot analysis of phospho-Akt (p-Akt), Akt , phospho-mTOR (p-mTOR), mTOR, phosho-S6 (p-S6), S6 and β-tubulin proteins of control (Ctrl) and ND5 mutated fibroblasts (Pat), with the relative quantification of p-mTOR and p-S6 levels. β-tubulin was used as loading control. (b) Immunoblot analysis of phospho-AMPK (p-AMPK), AMPK and β-tubulin protein level of control (Ctrl) and ND5 mutated fibroblasts (Pat), with the relative quantification of p-AMPK levels. β-tubulin was used as loading control. (c) Immunoblot analysis of p-AMPK, AMPK, MCU and β-tubulin protein level of control (Ctrl) and ND5 mutated fibroblasts (Pat). The blots are representative of 3 different experiments.*
*** P< 0.001.*

DISCUSSION – MITOCHONDRIAL DISEASES

In medical literature the term “mitochondrial disorders” defines a set of clinical syndromes associated with failure of mitochondria, in particular due to abnormalities of mitochondrial energy metabolism, namely oxidative phosphorylation. This crucial process is executed by five multi-protein complexes of the respiratory chain, localized in the inner mitochondrial membrane. Among them, complex I (NADH: ubiquinone oxidoreductase) is the largest.

During the last few decades, mutations in nuclear genes encoding structural subunits of complex I have been identified as a cause of multiple devastating encephalo-myopathies, often with early childhood onset.

There are several studies that underline the involvement of Ca^{2+} signaling in these disorders, which primarily depends on an increased ROS production in these cells, responsible for the subsequent loss of the mitochondrial membrane potential, and alteration in the organelle morphology (Willems et al., 2008) (Willems et al., 2009) (Valsecchi et al., 2009) (Distelmaier et al., 2009) (Valsecchi et al., 2010).

Our work is inserted in this line of research but presents some original and interesting aspects never considered in the previously published data. The first aspect of originality of our study is the experimental model: to study mitochondrial disorders, we utilized skin primary fibroblasts derived from complex I deficient patients with mutations in mitochondrial DNA and not in nuclear DNA. In particular, we focused our work on fibroblasts from a patient with a specific ND5 point mutation (13514A>G), who presented a relatively milder phenotype compared to what is normally reported for patients affected by mitochondrial disorders (Corona et al., 2001). This element caught our attention and suggested us the possible existence of a metabolic and molecular mechanism that could explain this milder phenotype, and that could help the identification of new potential therapeutical targets for other mitochondrial disorders.

Only recently, the involvement of autophagy in many physiological (Levine and Kroemer, 2008) and also pathological conditions (Ravikumar et al., 2010) started to emerge. However, there have been no studies about the role of autophagy in mitochondrial disorders. This represents another important novel element of our work.

Our findings indicated that in patient derived fibroblasts there is a higher number of autophagosomes already in basal conditions, compared to fibroblasts derived from healthy donor, as revealed by the accumulation of the LC3 marker (Mizushima et al., 2010) [*Figure 1*].

We then clearly demonstrated that this increase in autophagosome number depends on an enhanced autophagic flux rather than its block. We showed this by different approaches. Firstly, we treated fibroblasts with chloroquine, which neutralize the lysosomal pH, preventing the fusion of proteases and lysosome degradation, thus causing an artificial block of the autophagic flux and accumulation of autophagosomes in normal conditions. If the flux is already blocked, the chloroquine treatment should not cause any further increase in autophagosome number. As shown in *Figure 2*, chloroquine treatment induces a further increase in autophagosomes formation in patient derived fibroblasts, relative to basal conditional and relative to control fibroblasts.

Secondly, we used another autophagic marker, SQSTM1/p62, to verify the origin of autohagosome accumulation. As reported in the literature, SQSTM1/p62 contains an LC3-interacting motif as well as an ubiquitin binding domain, and appears to act by linking ubiquitinated substrates with the autophagic machinery (Bjorkoy et al., 2005). Thus the function of SQSTM1/p62 is shared between the ubiquitination and the autophagy processes. For this reason the interpretation of SQSTM1/p62 protein accumulation data is not straightforward. However, the SQSTM1/p62 mRNA transcriptional up-regulation unequivocally indicates when there is an increase of autophagic flux (Klionsky et al., 2012), and we demonstrated that this is the case in our ND5 fibroblasts [*Figure 3*].

In specific cases, the autophagy process is selectively direct to remove damaged organelles, and mitochondria, being the site of an intense biosynthetic activity, as well as the source of ROS production. Indeed, mitochondria are specific targets of the autophagic process through a selective mechanism called mitophagy (Geisler et al., 2010; Narendra et al., 2008; Pattingre et al., 2005; Suen et al., 2010).

We hypothesized that our ND5 fibroblasts model presents an adaptive and compensatory mechanism leading to the elimination of non-functional and damaged mitochondria and the restoration of the non-functional mitochondrial pool with new organelles, keeping in equilibrium the rate of mitochondrial clearance with the rate of mitochondrial biogenesis. Indeed, in mitochondrial disorders the mutated mtDNA co-exists intracellularly with wild-type mitochondrial genome in a condition known as "heteroplasmy".

Despite the apparent discrepancy of our data on the protein level of mitochondrial markers with our hypothesis [*Figure 4a*], when we induced a mild mitochondrial damage, there is significant acceleration of mitochondrial removal in mutated fibroblasts [*Figure 4b*], indicating that mitochondria are direct substrates of the increased autophagic flux.

This discrepancy could be explained with the presence of enhanced mitochondrial biogenesis in basal conditions, which could mask the increased mitophagy and could represent the compensatory mechanism of patient cells to maintain a pool of new functional mitochondria. This mechanism, by compensating the metabolic defects in mutated fibroblasts, could also explain other two important parameters, namely mitochondrial morphology and membrane potential, which show no difference between control and complex I deficient cells in our model. Moreover, the fact that mitochondria of ND5 fibroblasts seem to be more elongated than control, is in line with the commonly accepted mechanism of mitochondrial elongation during autophagy, which is fundamental for the maintenance of cellular ATP level (Gomes et al., 2011).

As the mitochondrial membrane potential is concerned, we did not record any depolarization in mutated fibroblasts after rotenone [*Figure 7a*], nor after oligomycin treatment (data not shown). This means that these cells are able to maintain the mitochondrial membrane potential, probably due to up-regulation of other respiratory chain complexes or, more likely, thanks to the efficient mitochondrial turnover that rapidly replaces non-functional mitochondria, thus compensating for the metabolic defects in our model.

Based on previously reported observations about the correlation between the intracellular Ca^{2+} signals and the regulation of autophagy (Cardenas et al., 2010) and taking advantage of the well-established expertise of our group in Ca^{2+} measurements (Granatiero et al., 2014; Pinton et al., 2007), we decided to investigate the role of Ca^{2+} homeostasis in complex I mutations, and in particular its involvement in the autophagy process. Overall, our data indicate that patient derived fibroblasts have a significant reduction in mitochondrial Ca^{2+} uptake, after agonist stimulation [*Figure 5*].

We further investigated the possible origin of this altered mitochondrial Ca^{2+} homeostasis in ND5 fibroblasts by looking at the distribution of ER-mitochondria contact sites, which recently emerged as a key feature of the modulation of mitochondrial Ca^{2+} uptake. Indeed, the rapid transport of Ca^{2+} into mitochondria after agonist stimulation is mainly due to the strategic location of the organelles that are in close contact with the ER, and thus sensing microdomains of high Ca^{2+} concentration (Rizzuto et al., 1993; Rizzuto et al., 1998; Rizzuto et al., 1992). Interestingly, we found defect in the spatial arrangement of ER-mitochondria contact sites, indeed, in our ND5 mutated cells there is a lower number of them [*Figure 7e*], despite the fact that both mitochondrial and ER morphology are not compromised.

Considering the molecular mechanism responsible for the ER-mitochondria tethering, Mitofusin2 (MFN2) has been identified as the first and most important mammalian protein to directly bridge the two organelles. MFN2 is localized on both the surface of the ER and on the outer mitochondrial membrane (OMM), and enriched in the ER–mitochondria interface,

where it directly connects ER with mitochondria via protein-protein interactions between MFN2 in the ER and MFN1 or MFN2 present in the OMM (de Brito and Scorrano, 2008).

In line with this, we demonstrated that ND5 mutated fibroblasts show a lower level of MFN2 protein [*Figure 7f*], which could explain the observed impairment in ER-mitochondria tethering.

Altogether our results suggest a possible correlation between the decrease in mitochondrial Ca^{2+} uptake and the increase in autophagic flux observed in ND5 mutated fibroblasts. In order to verify if the manipulation of Ca^{2+} dynamics could directly affect the autophagic response in our complex I deficiency model, we took advantage of the molecular identification of the protein responsible of Ca^{2+} entry in mitochondria, namely MCU, obtained in our laboratory few years ago (De Stefani et al., 2011). We overexpressed MCU in order to increase mitochondrial Ca^{2+} uptake in the patient cells. As expected, overexpression of MCU produces a complete restoration of mitochondrial Ca^{2+} uptake to control level in mutated fibroblasts [*Figure 8a*], and more interestingly, leads to a significant reduction in the autophagosome number [*Figure 8b*]. This suggests that mitochondrial Ca^{2+} can regulate autophagy.

Additionally, our analysis of the signaling pathways involved in the establishment of ND5 cell phenotype confirmed the involvement of AMPK in the correlation between autophagy and intracellular Ca^{2+} handling [*Figure 9*], as previously reported in the literature (Cardenas et al., 2010).

The capacity of mitochondrial Ca^{2+} homeostasis to directly control the autophagy induction and the cell protection against apoptosis in our cellular model opens the route for the development of new therapeutic approaches based on the fine regulation of intracellular Ca^{2+} dynamics. It is possible that the manipulation of MCU activity could thus relieve and ameliorate the phenotype of patients affected by mitochondrial disorders.

RESULTS – NEURODEGENERATION

Neurodegenerative diseases are a large and heterogeneous group of disorders characterized by selective and progressive death of specific neuronal subtypes. Ca^{2+} is the main signaling molecule that regulates neuronal activities such as synaptic transmission, plasticity and neurite outgrowth. In addition, intracellular Ca^{2+} homeostasis has been shown to play a key role in the control of cell fate, by impinging on cell death and survival pathways, so it is not surprising that the impairment of Ca^{2+} signaling always precedes neurodegeneration (Duchen, 2012; Pivovarova and Andrews, 2010; Rizzuto et al., 2012).

Keeping in mind that the mitochondrial Ca^{2+} accumulation could trigger apoptosis, we wanted to investigate the role of mitochondrial Ca^{2+} loading, induced by MCU overexpression, in the pathogenesis of neurodegenerative disorders.

As model for this study, we decided to use mouse primary cortical neurons cultured from newborn (P0-P2) C57BL6 mice as described in the methods section.

MCU overexpression enhances mitochondrial Ca^{2+} uptake in primary cortical neurons

Firstly we wanted to analyze the cellular Ca^{2+} homeostasis in our primary neurons in response to the overexpression of the Ca^{2+} uniporter.

It has been already demonstrated that the overexpression of mitochondrial Ca^{2+} uniporter, MCU, in HeLa cells induces an increase of mitochondrial Ca^{2+} uptake (De Stefani et al., 2011), and we wanted to know if a similar increase in mitochondrial Ca^{2+} uptake is measured also in our model.

To perform our experiments, we took advantage of the last generation cameleon probe, specifically targeted to mitochondria, 4mtD1cpV(Palmer and Tsien, 2006). We co-transfected

primary cortical neurons with this 4mtD1cpV cameleon probe and plasmid coding for MCU or empty vector as control. Primary neurons were then stimulated with a high concentration of K^+ to induce plasma membrane depolarization, resulting in a raise of intracellular Ca^{2+}, and the cpVenus/CFP probe fluorescence ratio was recorded.

MCU-overexpressing neurons showed a higher increase in the probe signal relatively to control neurons, indicating that they had a higher mitochondrial Ca^{2+} uptake capability [*Figure 10*].

In conclusion, the overexpression of the mitochondrial Ca^{2+} uniporter perturbs mitochondrial Ca^{2+} handling, increasing the Ca^{2+} entry in primary cortical neuron.

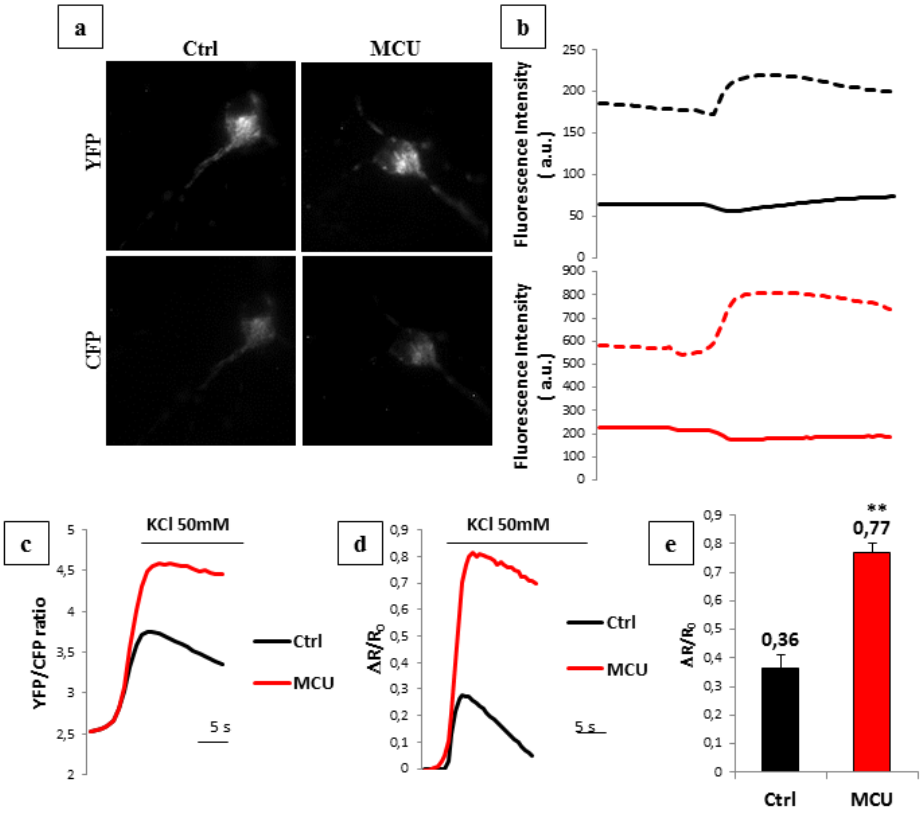

Figure 10: <u>MCU overexpression enhances mitochondrial Ca^{2+} uptake in primary cortical neurons.</u> *(a) Representative images of YFP and CFP fluorescence of mouse primary cortical neurons co-transfected with 4mtD1cpv cameleon probe and either empty vector pcDNA as control (Ctrl) or MCU-flag-pcDNA (MCU). (b) Intensity plots of YFP (dotted line) and CFP (solid line) cameleon fluorescence in control (black) and MCU-overexpressing neurons (red), after KCl depolarization (50mM). (c) Representative traces of YFP/CFP ratio in Ctrl and MCU, after KCl depolarization (50mM). (d) Representative traces of $\Delta R/R_0$ ratio in Ctrl and MCU neurons, after KCl depolarization (50mM). (e) Relative quantification of $\Delta R/R_0$ ratio represented in (d). The measurements were performed at least for 30 samples from 6 different experiments. ** P< 0.001.*

MCU overexpression induces mitochondrial fragmentation

Mitochondria are highly dynamic organelles and undergo continues changes in shape and size thanks to the alternation of fission and fusion events. Since the first evidence by Martinou et al. and the contribution of several subsequent studies (Martinou et al., 1999; Montero et al., 2000; Pivovarova et al., 1999), it is widely accepted that there is a strong association between neuronal cell death and mitochondrial morphology alteration. We thus decided to investigate the mitochondrial morphology in our system and to study the effect of manipulation of Ca^{2+} dynamics on mitochondrial network distribution.

In order to do this, we co-transfected mouse primary cortical neurons with a red fluorescent probe specifically targeted to mitochondria (mtRFP) and either empty vector as control or MCU-coding plasmid to overexpress the Ca^{2+} uniporter.

Confocal microscope analysis of RFP fluorescence showed a clear alteration of mitochondrial morphology in MCU-overexpressing neurons, with fragmentation in the soma and nearly complete disappearance of mitochondria in dendrites. Control cells present a normal mitochondrial network, characterized by elongated mitochondria in both soma and dendrites. These experiments demonstrated that the overexpression of the mitochondrial Ca^{2+} uniporter induces mitochondrial fragmentation in primary neurons.

The same experimental approach was used to study the effect of an excitotoxic stimulus, namely an excess of glutamate. Glutamate is the major excitatory neurotransmitter in the brain, but the exposure of central neurons to excessive glutamate leads to excitotoxic cell death (Choi, 1992; Olney and Sharpe, 1969).

We thus evaluated the mitochondrial morphology in control and in MCU-overexpressing neurons, before and after an excess of glutamate treatment. As expected, glutamate treatment promotes mitochondrial fragmentation in control neurons, which is a well-recognized sign of the induction of cell death. Interestingly, this phenotype is already present in MCU-overexpressing neurons, in basal conditions and it is even further exacerbated after glutamate

treatment. This indicates that MCU-induced increase in mitochondrial Ca^{2+} is directly correlated with an higher susceptibility of neurons to cell death [*Figure 11*].

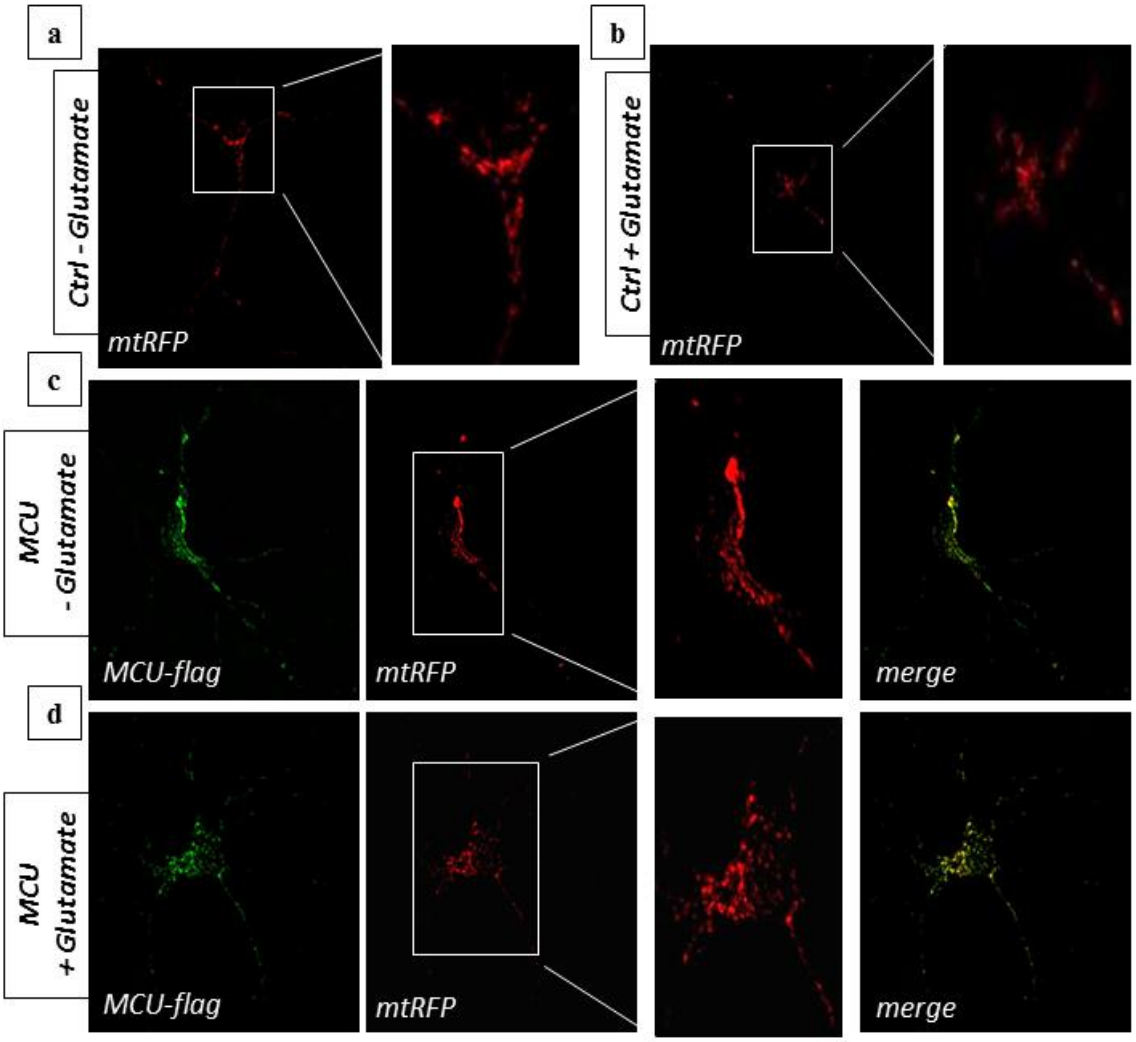

Figure 11: ***<u>MCU overexpression induces mitochondrial fragmentation.</u>*** *Detection of mitochondrial RFP fluorescence in primary cortical neurons co-transfected with mtRFP and empty vector pcDNA (Ctrl), without (a) or with glutamate treatment (100μM for 1 hour) (b). Immunofluorescence analysis with anti-flag antibody of cortical neurons co-transfected with mtRFP and MCU-flag-pcDNA (MCU), with (d) or without glutamate treatment (100μM for 1 hour) (c). Insets represent high magnification of the neuronal soma. Were analyzed at least 30 cells, from 3 different experiments for each condition.*

<u>MCU overexpression impairs neurons survival</u>

We produced new adenoviral vectors for MCU expression in primary neuronal cultures, in order to combine the high infection efficiency of adenovirus and the possibility to insert a

tissue-specific promoter (synapsin) to direct the expression selectively in neuronal cells (see Materials and Methods for more details).

Using this new tool, we explored the direct involvement of the mitochondrial Ca^{2+} uniporter in the induction of neuronal cell death in our model.

The percentage of infected cells, identified as GFP positive cells, significantly and progressively decreased over time in MCU-overexpressing neuron, while control cells did not show any GFP-positive cell loss [*Figure 12*]. This points out a direct effect of MCU expression in inducing cell death in primary neurons.

The possibility that the decreased number of MCU-GFP positive cells might be due to apoptosis is currently under investigation.

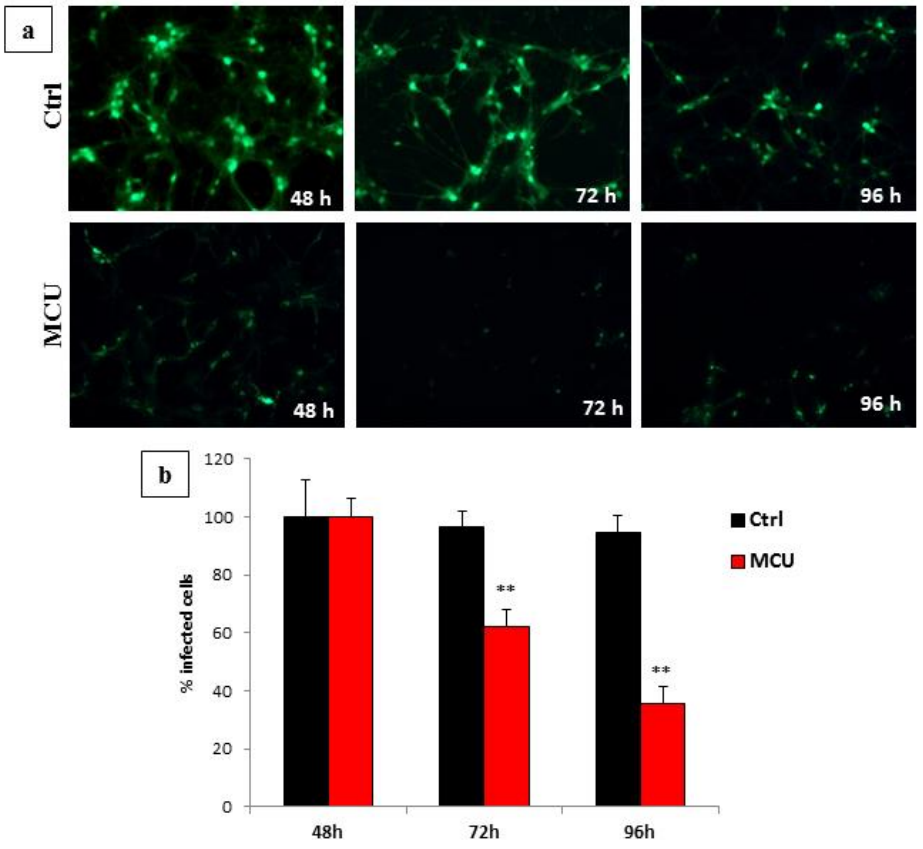

Figure 12: ***<u>MCU overexpression impairs neurons survival.</u>*** *(a) Detection of GFP fluorescence in primary cortical neurons infected with synapsin-driven pEGFP (Ctrl) or MCU-GFP (MCU) adenoviral vectors, at 48 – 72 - 96 hours from the infection. (b) Relative quantification of GFP-positive primary neurons in control (Ctrl) [100% - 96% - 95%] and MCU-overexpressing (MCU) [100% - 62% - 36%] samples, as presented in (a). Were analyzed 60 random fields for each condition, from 3 different experiments. ** P< 0.001.*

MCU-overexpression accelerates the loss of mitochondrial membrane potential in primary neurons

Taking into account the findings we obtained until this point, we decided to further investigate if the mitochondrial Ca^{2+} uniporter could be directly implicated in the excitotoxicity process.

The alteration of mitochondrial membrane potential is one of the earliest events in response to excitotoxicity insults (Ankarcrona et al., 1995; Pereira and Oliveira, 2000; Ward et al., 2000), thus we decided to measure the mitochondrial membrane potential in primary cortical neurons overexpressing MCU.

We utilized the Tetra-Methyl-Rhodamine-Methyl Ester (TMRM) probe to monitor mitochondrial membrane potential in mouse primary cortical neurons infected with either synapsin-driven pEGFP (synGFP) or MCU-GFP (synMCU-GFP) adenoviral vectors, after 48 hours from infection. We measured the mitochondrial membrane potential in resting conditions and after addition of excess of glutamate, to induce excitotoxicity.

MCU-overexpressing neurons showed a great acceleration in the rate at which they lose the mitochondrial membrane potential following the excitotoxic stimulus [*Figure 13b and c*]. This means that MCU overexpression, after excitotoxic insults, sensitized primary neurons to mitochondrial membrane potential loss.

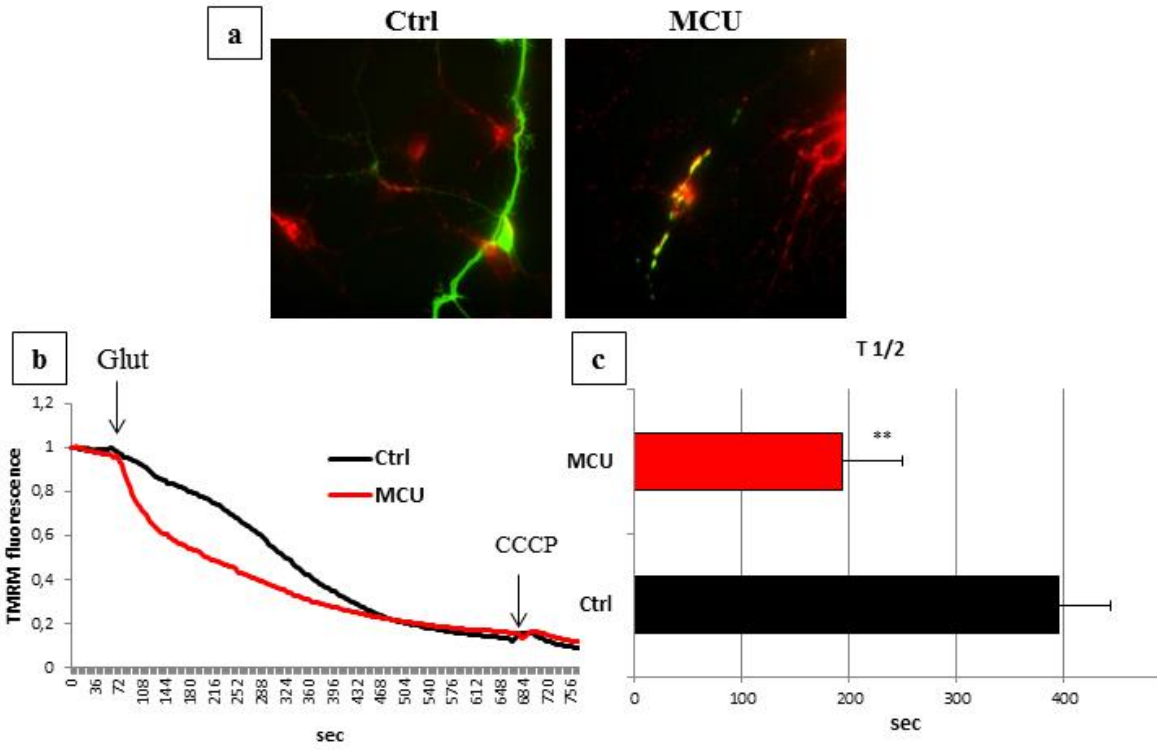

Figure 13: ***<u>MCU-overexpression accelerates the loss of mitochondrial membrane potential in primary neurons.</u>*** *(a) Representative images of primary cortical neurons infected with either synapsin-driven pEGFP (Ctrl) or MCU-GFP (MCU) adenoviral vectors for 48 hours and loaded with TMRM probe (20nM for 30 minutes). (b) Representative traces of mitochondrial membrane potential in control and MCU-overexpressing primary neurons, after excess of glutamate (100μM) and CCCP (10μM). (c) Relative quantification of the half-time of the TMRM fluorescence loss in Ctrl (392.2 ± 55.3 sec) and MCU-overexpressing neurons (194.4 ± 14.3 sec). The measurements were performed at least for 30 samples from 3 different experiments. ** P< 0.001.*

<u>MCU-overexpression elevates cytosolic Ca^{2+} inducing excitotoxicity</u>

It has been previously reported that excitotoxicity is mediated by elevation of cytosolic Ca^{2+}, and that the rate of cell death correlates with the absolute amount of Ca^{2+} taken up (Carriedo et al., 1998; Eimerl and Schramm, 1994; Hartley et al., 1993).

Therefore we decided to monitor the cytosolic Ca^{2+} levels, using the low-affinity ratiometric Fura-FF probe, in mouse primary cortical neurons, infected with synGFP or synMCU-GFP adenovirus after treatment with an excess of glutamate.

MCU-overexpressing neurons showed a higher free Ca^{2+} level in basal conditions compared to control neurons. In addition, after exposure to an excess of glutamate, they presented a progressively higher and faster increase in Ca^{2+} level respect to control cells [*Figure 14*].

These experiments are consistent with the data we obtained before, indicating the presence of a higher sensitivity to the induction of cell death in cells overexpressing MCU.

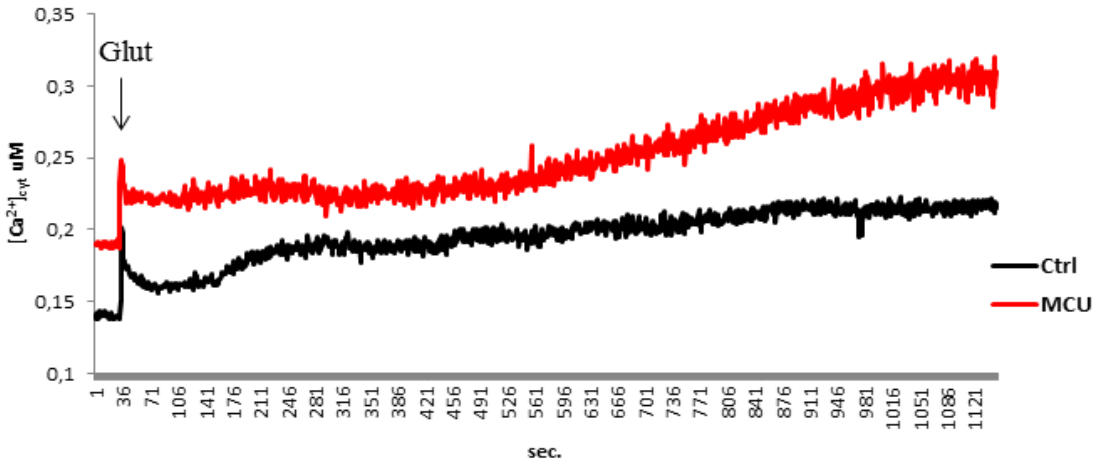

Figure 14: ***<u>MCU-overexpression elevates cytosolic Ca^{2+} inducing excitotoxicity.</u>***
*Representative traces of cytosolic Ca^{2+} concentration of mouse primary cortical neurons, infected with either synapsin-driven pEGFP (Ctrl) or MCU-GFP (MCU) adenoviral vectors for 48 hours, after addition of excess of glutamate (100μM), measured by Fura-FF probe (5mM for 20 minutes of incubation). The measurements were performed at least for 18 samples from 3 different experiments. ** P< 0.001.*

<u>*MCU-overexpression* in vivo *induces brain tissue degeneration*</u>

Lastly, we wanted to confirm our data in an *in vivo* model using a stereotaxic injection, in order to precisely infuse MCU-coding viral vector in the midbrain of C57BL6 mice.

Immunofluorescence analysis of brain sections of the injected area revealed the presence of GFP-infected control cells with a normal cellular morphology. On the contrary, the MCU-positive neurons have a clear alteration in cellular morphology [*Figure 15*], suggesting cell damage or cell death. The characterization of the phenotype of these infected cells is currently under investigation in our laboratory, by the analysis of specific neurodegeneration markers.

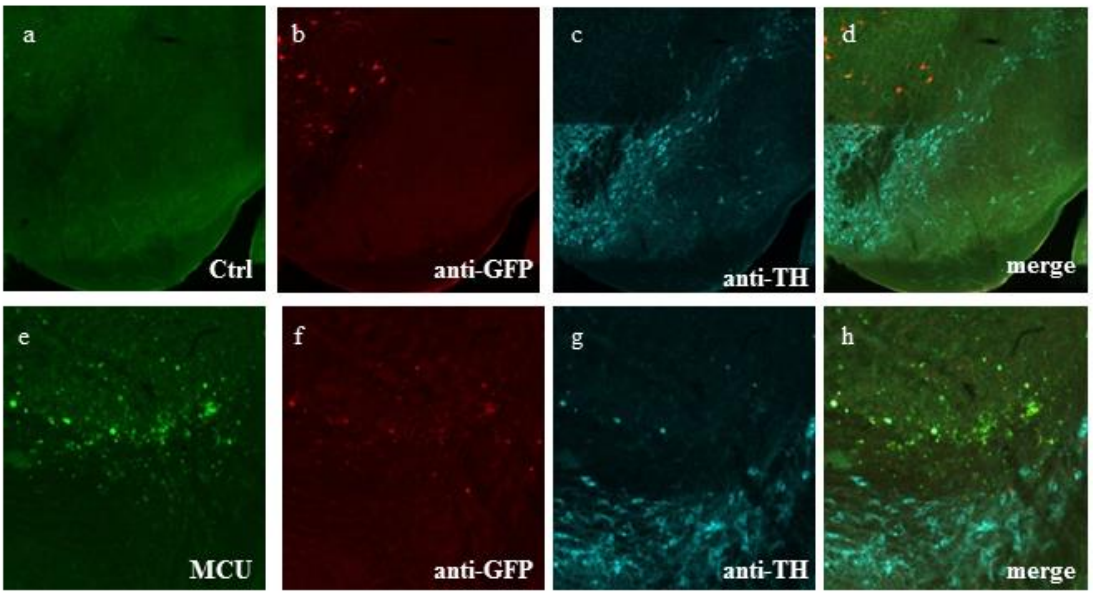

Figure 15: <u>MCU overexpression</u> in vivo induces brain tissue degeneration. *Detection of GFP fluorescence in primary cortical neurons, after midbrain stereotaxic injection with either synapsin-driven pEGFP (Ctrl) (a) or MCU-GFP (MCU) (e) adenoviral vectors after 14 days from the injection. Immunofluorescence analysis with anti-GFP and anti-Tyrosine Hydroxylase (TH) antibodies, and overlay of three wavelengths of Ctrl (b-c-d) and MCU (f-g-h) injected midbrain area.*

DISCUSSION – NEURODEGENERATION

Neurodegenerative disorders are debilitating diseases of the brain, characterized by behavioral, motor and cognitive impairments. Neuronal activity is mainly triggered by the stimulation of plasma membrane channels and the initial Ca^{2+} entry is subsequently modulated by the activity of intracellular Ca^{2+} stores (Clapham, 2007). In particular, Ca^{2+} uptake and release by endoplasmic reticulum (ER) and mitochondria plays essential role in the modulation of Ca^{2+} signaling, integrating cellular responses to a wide variety of external stimuli.

Mitochondrial Ca^{2+} signaling is fundamental in the central nervous system. Neuronal mitochondria are able to accumulate a large amount of Ca^{2+}, representing a striking example of the complexity and pleiotropicity of Ca^{2+} signaling; they are essential for cellular bioenergetics, organelle communication and organelle dynamics and trafficking. In addition, as already discussed, they could also play an important role in the pathological alterations in human disorders. There is considerable evidence underlining the involvement of mitochondria in the pathogenesis of several neurodegenerative disorders, but not limited to Parkinson's disease, Alzheimer's disease and Huntington's disease (Bezprozvanny, 2009; Gibson et al., 2010).

Thus, understanding the mechanism of neuronal dysfunction and death represents a major frontier in contemporary medicine.

The recent identification in our laboratory of the long sought-after mitochondrial Ca^{2+} uniporter (MCU) (De Stefani et al., 2011), which is responsible of the Ca^{2+} entry in mitochondria, has opened the possibility to directly study the implication of this channel in the pathogenesis of neurodegeneration. In the seminal work of De Stefani et al. it was demonstrated that the overexpression of MCU in HeLa cells leads to an increase in

mitochondrial Ca^{2+} uptake. Similarly, we demonstrated in this thesis that in a physiological neuronal system (mouse primary cortical neurons), the overexpression of this channel has a similar effect [*Figure 10*]. Our attention was caught by the surprising difference in the mitochondrial morphology reported in studies performed in primary cortical neurons compared to cell lines. Indeed, in our primary culture model, the mitochondria of MCU-overexpressing neurons are clearly fragmented [*Figure 11*].

It is reported in the literature that the loss of mitochondrial membrane potential and the subsequent alteration in mitochondrial morphology is one of the first signs of neuronal suffering (Martinou et al., 1999). This suggests that MCU-overexpression could have an effect in triggering neuronal cell death.

With the proceeding of our work, we faced two main issues of our experimental model: one is that primary cultures are mixed cultures, composed by available proportion of different cell populations, like neurons, astrocytes, microglia and others, while we were only interested in neurons, and second is the extremely low efficiency of neuronal transfection with common plasmid vectors. For these reasons, we worked to produce a new expression system for MCU expression, based on adenoviral vector with a neuron-specific promoter, synapsin. This new tool permitted us to perform some decisive and important experiments to demonstrate that the overexpression of MCU in neurons makes them more sensitive to cell death. In particular, we measured the loss of mitochondrial membrane potential [*Figure 13*] and the cytosolic Ca^{2+} concentration [*Figure 14*] in mouse primary cortical neurons, after an excitotoxic stimulus, namely the excess of glutamate. Glutamate is a physiological excitatory neurotransmitter, but exposure of central neurons to excessive glutamate stimulation leads to excitotoxic death (Choi, 1992; Olney and Sharpe, 1969). Indeed, our data clearly demonstrate that MCU overexpression enhances the effect of excitotoxic treatment in primary neurons, since membrane potential loss is accelerated and cytosolic Ca^{2+} increases faster in MCU-infected neurons, compared to control neurons.

Overall our results agree with the data published in the meanwhile on the role of MCU in excitotoxicity (Qiu et al., 2013). However, our work presents some elements of novelty respect the work described by Qiu and collaborators. Indeed, we went further in the study of the physio-pathological role of MCU in neurodegeneration, analyzing it also in an *in vivo* system.

For these experiments, we directly injected MCU synapsin-driven adenovirus in the midbrain area of adult mice, by stereotaxic injection and we evaluated the alterations in cellular morphology of MCU-infected neurons [*Figure 15*]. MCU overexpression caused evident cell damage and tissue degeneration in the injected areas. Obviously, these *in vivo* results are preliminary and we aim to consolidate them with additional analysis of the effect of MCU overexpression with specific neurodegeneration cellular markers.

In conclusion, we developed both *in vitro* and *in vivo* systems that represent useful tools for research in the neurodegeneration field. In addition, we discovered a crucial role for MCU in the pathogenesis of neurodegeneration, opening the door to possible clinical intervention through the regulation of intracellular Ca^{2+} signaling and, in particular, through the modulation of mitochondrial Ca^{2+} uptake.

Cell culture, transfection and proteomic analysis

- The "mitochondrial diseases" experiments were performed on primary skin fibroblasts derived from healthy (without mutations on complex I) and mutated (point mutation on ND5 subunit of complex I, specifically 13514A>G) patients. Primary fibroblasts were cultured in Dulbecco's modified Eagle's medium (DMEM) (Life Technologies), supplemented with 20% Fetal Bovine Serum (FBS) (Life Technologies), containing penicillin (100 U/ml) and streptomycin (100 μg/ml).

- The "neurodegeneration" experiments were performed on primary cortical neurons from p0-p2 newborn C57BL6 mice. Specifically, the brain cortex of newborn mice were extracted using a stereomicroscope and digested with trypsin at 37°C for 10 minutes. After several digestion steps, the obtained cells are seeded on glasses coverslips, previously incubated with Poli-Lysine and cultured in MEM (Life Technologies), supplemented with 10% Horse Serum (Life Technologies), N2 supplement (Life Technologies), B27 supplement (Life Technologies), Sodium Pyruvate (Life Technologies), Biotin, Glucose, L-Glutamine, penicillin and streptomycin. The primary neurons were cultured in this complete MEM for 6 DIV before transfection or infection.

- Both human skin primary fibroblasts and mouse primary cortical neurons were seeded on glasses coverslips, just before the transfection procedure cells were washed with complete medium without antibiotics and they were transfected with a standard Lipofectamine 2000 (Life Technologies) protocol. In particular, for 13 mm coverslips were prepared two tubes, on one hand optimem medium (Life Technologies) plus totally 0.8μg DNA, and on the other hand, optimem plus 2μl of lipofectamine 2000 reagent. After five minutes they are mixed, after other 20 minutes 100 μl of this solution were added to the cell monolayer and incubated

for 3 hours. Then the medium were changed with fresh one (N.B.: for primary cortical neurons were added half of the original cultured medium, containing growth factors and specific nutrients). The experiments were carried out 24 hours after transfection. For one 24 mm coverslip the amount of solution and DNA amount is multiplied 4 times; while for 10 cm dishes multiplied 10 times.

- For glucose and serum deprivation experiments (starvation condition) culture medium were washed four times and then cells were incubated for 4 hours in Krebs–Ringer modified buffer (KRB: 135 mM NaCl, 5 mM KCl, 1 mM $MgSO_4$, 0.4 mM K_2HPO_4, 20 mM HEPES, pH=7.4) plus 1mM $CaCl_2$. This solution was sterilized by filtration using 0.22 μm filters.

- For chloroquine treatment we challenged the fibroblasts with 50μM chloroquine at different time points (20 – 60 – 90 – 105 – 135 – 180 minutes). Among them we have chosen 60 minutes of treatment.

- Cells were lysated in RIPA buffer (150 mM NaCl, 50 mM Tris, 1 mM EGTA, 1% Triton X-100), supplemented with proteases and phosphatase inhibitors cocktail (Roche) for 30 minutes freeze-thaw procedure. After BCA quantification, 25 μg of total proteins were separated by SDS-PAGE gel electrophoresis in 4-12% SDS bis-tris, acrylamide gels (Life Technologies), transferred to Nitrocellulose membrane (Life Technologies) 0,4μm pore, stained with Ponceau S solution and immunoblotted against different antidody.

In particular: SQSTM1/p62 (1:1000); MICU1 (1:1000); MCU (1:1000) were purchased from Sigma-Aldrich. Tom20 (1:2000); Hsp60 (1:1000); Actin (1:5000); β-tubulin (1:5000) were purchased from Santa Cruz Biotechnologies. p-AMPK (1:1000); AMPK (1:1000); p-mTOR (1:1000); mTOR (1:1000); p-Akt (1:1000); Akt (1:1000); p-S6 (1:1000); S6 (1:1000) were purchased from Cell Signaling. Cytocrome c (1:1000); AIF (1:1000) SDHA (1:1000) from BD.

Secondary HRP-conjugated antibodies (1:5000) were purchased from BioRad.

All chemicals were purchased from Sigma-Aldrich, unless specified.

- The MCU-flag/pcDNA expression construct were provided by De Stefani et al. 2011 (De Stefani et al., 2011).

Adenovirus production

Working with mouse primary cortical neurons we faced two main issues: one is that are mixed cultures and we were only interested in neurons, and second the low efficiency of transfection with common plasmid vectors. Thus we worked to produce a new vector for MCU expression which is an Adenovirus with the neuron-specific promoter, synapsin.

Recombinant adenoviruses provide a versatile system for gene expression studies.

In order to introduce the gene of interest in adenovirus, we used AdEasy System (He et al., 1998). In our case, synapsin-pEGFP or synapsin-MCU-GFP, are firstly cloned into a shuttle vector, e.g. pAdTrack. The resultant plasmid is linearized by digesting with restriction endonuclease Pme I, and subsequently co-transformed into E. coli. BJ5183 cells with an adenoviral backbone plasmid, e.g. pAdEasy-1. Recombinants are selected for kanamycin resistance, and recombination confirmed by restriction endonuclease analyses. Finally, the linearized recombinant plasmid is transfected into adenovirus packaging cell lines, e.g. 293 HEK cells. Recombinant adenoviruses are typically generated within 7 to 12 days.

When the HEK 293 cells are completely transfected, we collected the cells, lysate them with 5 freeze-thaw cycle, pelleted and, using the supernatant, we infected other HEK 293 cells in order to amplify it. The last lysis was performed in Tris 10mM CaCl2 pH 8 and then aliquoted and stored at -20°C.

For the stereotaxic injection, the same viruses were further purified after the amplification step, using Cesium Chloride gradient, and two subsequent centrifugations.

After the virus purification, we obtained stocks of Adenoviral vector, synapsin promoter, coding for pEGFP with viral titer 6.32x10^10 PFU/ml and for MCU-GFP with viral titer 4.76x10^10 PFU/ml. Starting from these stocks solutions we injected 1μl of them per mouse,

injecting 6.32x10^7 PFU and 4.76x10^7 PFU, respectively of pEGFP and MCU-GFP per mouse.

Aequorin Ca^{2+} measurements

Aequorin is a 22 KDa photoprotein isolated from jellyfish *Aequorea Victoria* which emits blue light in the presence of Ca^{2+}. In its active form the photoprotein includes an apoprotein and a covalently bound prosthetic group, coelenterazine. The apoprotein contains four helix-loop-helix "EF hand" domains, three of which are Ca^{2+}-binding domains (Inouye and Tsuji, 1993). These domains confer to the protein a particular globular structure forming the hydrophobic core cavity that accommodates the ligand coelenterazine. When Ca^{2+} ions bind to the three high affinity EF hand sites, coelenterazine is oxidized to coelenteramide, with a concomitant release of CO_2 and emission of light (Head et al., 2000). Reconstitution of an active aequorin, expressed recombinantly, can be obtained also in living cells by simple addition of coelenterazine into the medium.

The possibility of using aequorin as Ca^{2+} indicator is based on the existence of a well characterized

relationship between the rate of photon emission and the $[Ca^{2+}]$. The first method used to correlate the amount of photons emitted to the $[Ca^{2+}]$, was that described by Allen and Blinks (Allen and Blinks, 1978). This mathematical approach reposes on an accurately relationship between $[Ca^{2+}]$ and the alogarithm of L/Lmax, where L is the instant rate of light emission and Lmax is the maximal values of light emission measured in saturated conditions. For the native jellyfish photoprotein, in this logarithmic scale the response are linear in the physiological range of cytosolic $[Ca^{2+}]$, i.e. between 10^7 and 10^5, thus allowing careful calibration of the luminescence signal into absolute $[Ca^{2+}]$ values.

Aequorin began to be widely used when the cDNA encoding the photoprotein was cloned, and also opened the possibility of molecular engineering the protein sequence; introducing

specific targeting sequences and thus directing the Ca^{2+} probe to a defined subcellular compartment (Garcia-Bustos et al., 1991; Hartl et al., 1989; Nothwehr and Gordon, 1990).

The aequorin detection system is derived from Cobbold and Lee description (Cobbold and Bourne, 1984) and is based on the use of a low noise photomultiplier placed in close proximity (2-3 mm) of aequorin expressing cells. The cell chamber, which is on the top of a hollow cylinder, is adapted to fit 13 mm diameter coverslips. Cells are continuously perfused via peristaltic pump with medium thermo stated at 37°C. The photomultiplier (Hamamatsu H7301) is kept in a dark box. The output of the amplifier-discriminator is captured by C8855-01 photon counting board in an IBM compatible microcomputer and stored for further analysis.

EXPERIMENAL PROCEDURES

- Cytosolic Ca^{2+}: Healthy and mutated primary fibroblasts were transfected with the cytAEQ construct (Brini et al., 1995), using Lipofectamine 2000 (see before the protocol). After 24 hours of transfection, 2 hours before the experiment, we reconstituted the protein by adding the prosthetic group, coelenterazine WT (Molecular Probe). Cells were perfused with modified KRB. In the first part of the measurement, the background signal is determined. In basal conditions the variations of $[Ca^{2+}]$ are very little (0.1-0.5μM), then we perfused KRB with histamine 100 μM, which is an agonist coupled via G proteins able to induce the generation of GAG and IP3, and thus the release of Ca^{2+} from the ER. In this way it is possible the induction of transient stimulation of Ca^{2+}, visible during the experiments by a transient peak. Then the amount of Ca^{2+} return to the background level, the total content of aequorin is estimated by discharging the remaining pool. This is achieved by perfusing a hypotonic Ca^{2+}-rich solution (10mM $CaCl_2$ in H_2O), that release aequorin into a Ca^{2+}-rich environment, in this way it is possible evaluate the Lmax.

- Mitochondrial Ca^{2+} uptake in intact cells: Healthy and mutated primary fibroblasts were transfected with the mtAEQ mutated construct (Rizzuto et al., 1992), using Lipofectamine

2000 (see before the protocol). After 24 hours of transfection, about 2 hours before the experiment, we reconstituted the protein by adding the prosthetic group, coelenterazine WT. For the experimental protocol the steps are: evaluation of the stable background, perfusion of histamine 100μM as agonist to visualize the Ca^{2+} transient, when the amount of Ca^{2+} comes back to the background level, perfusion of digitonin solution to estimate Lmax.

- Mitochondrial Ca^{2+} uptake in permeabilized cells: this experiment allows evaluating the characteristic of mitochondrial Ca^{2+} uptake machinery independent to ER Ca^{2+} release and the formation of microdomains of high [Ca^{2+}] in close proximity to mitochondrial Ca^{2+} channel. Healthy and mutated primary fibroblasts were transfected with the mtAEQ mutated construct, using Lipofectamine 2000 (see before the protocol). After 24 hours of transfection, 2 hours before the experiment, we reconstituted the protein by adding the prosthetic group, coelenterazine WT.

Measurement in digitonin-permeabilized cells is performed perfusing cells in Intracellular Buffer (IB: KCl 130mM, NaCl 100mM, K_2PO_4 20mM, Hepes 200mM, Succinic Acid 50mM, Malic Acid 10mM, Pyruvate 10mM, $MgCl_2$ 10mM, pH 7.0 with KOH) for 60 seconds. Cells are then perfused with the same buffer with 20μM digitonin for 60 second and washed with IB buffer for other 60 second. Then we perfused a known [Ca^{2+}] solution, specifically containing 2mM $CaCl_2$. In this way it possible evaluate the Ca^{2+} peak and its kinetic.

- Endoplasmic Reticulum Ca^{2+} amount and release: Healthy and mutated primary fibroblasts were transfected with the erAEQ construct (Montero et al., 1995), using Lipofectamine 2000 (see before the protocol). The ER [Ca^{2+}] is very high, between 200 and 500μM, for this reason it is necessary to empty the store before the reconstitution. After 24 hours of transfection, the cells were incubated in KRB supplemented with EGTA 600μM and the Ca^{2+} ionophore ionomycin 1μM. The reconstitution is performed with coelenterazine n (low affinity). After the reconstitution, the ionophore were removed by washing the cells three times with a KRB solution with BSA2% and EGTA 2mM. The experiment starts placing the

coverslip in the chamber and perfusing the KRB with 100μM of EGTA in order to maintain a low [Ca^{2+}] in the store. At the beginning of the experiments, an additional prolonged wash (200 sec) with KBR/BSA/EGTA is carried out. At this point, the medium is replaced with KRB containing a specific [Ca^{2+}], in general 1mM $CaCl_2$, to observe an increase in [Ca^{2+}] until the achievement of plateau level that represents the resting ER [Ca^{2+}]. At this point, KRB supplemented with histamine 100μM is added, appreciating the kinetic of Ca^{2+} release from the ER. As for the other aequorin experiments, the use of digitonin solution at the end allows to estimate Lmax.

FRET Ca^{2+} measurements

Cameleons are FRET-based ratiometric Ca^{2+} probe. The molecular structure is based on two variant of GFP (having differing excitation and emission characteristics), calmodulin (CaM), and the calmodulin-binding domain of myosin light chain kinase (M13). It was created by Roger T. Tsien and coworkers (Palmer and Tsien, 2006). The excitation energy of one fluorophore (the donor) is transferred to another (the acceptor) by dipolar interactions, without fluorescence emission (FRET). The donor emission and acceptor absorption spectra must overlap for FRET to occur. Calmodulin is able of bind Ca^{2+} ions and the M13 chain can bind with calmodulin after it has bound the Ca^{2+} ions. The binding of Ca^{2+} by the calmodulin moiety of cameleon produces a conformational change of the entire molecule and the consequent positions of the two fluorescent proteins into close spatial proximity. In this conformation, dipolar energy transfer by the excited donor protein stimulates the acceptor to produce secondary fluorescence. Intracellular [Ca^{2+}] can be determined by fluorescence ratio imaging. Also cameleon based probe can be targeted into different intracellular compartment. In our experiments we used mitochondrially-targeted cameleon. The GFP variants used are CFP (the donor) and cpVenus (the acceptor).

Mouse primary cortical neurons were grown on 24 mm glasses coverslips (previously pre-treated with L-poly-lisine) and transfected, after 6 DIV, using Lipofectamine 2000 (see before) with 4mtD1cpv as probe, and with either empty pcDNA vector for control or MCU-flag/pcDNA for the MCU-overexpression (1.5 μg 4mtD1cpv : 2.5 μg pcDNA or MCU-flag/pcDNA). The transfection solution was maintained under the cells for 3 hours and then the medium was changed with half of original medium. 24 hours after transfection, primary neurons were mounted into an open-topped chamber and maintained in KRB, experiments were started in 1 mM $CaCl_2$; after addition of EGTA 2mM, to chelate external Ca^{2+}, cells were stimulated by applying KCl 50mM; thereafter, Ca^{2+} ionophore ionomycin were applied to completely discharge the stores and finally a saturating $CaCl_2$ concentration (5μM) is added (plus TRIS-HCl 10 mM to avoid acidification) in order to verify the dynamic range of each probe.

Image analysis was performed by the public domain Fiji program (developed at the U.S. National Institutes of Health by Wayne Rasband and available on the Internet at http://rsb.info.nih.gov/ij/).

YFP and CFP images were subtracted of background signals and distinctly analyzed after selecting proper regions of interest (ROIs) on each cell (identified based on their morphology).

Subsequently, a ratio between cpVenus and CFP emission was calculated. Data are presented as normalized ratio for 4mtD1cpv or for the ratio difference between the starting point (R_0) and the point reach after depolarization (R) ($\Delta R/R_0$). Cells expressing the fluorescent probes were analyzed using an inverted Zeiss Axiovert 100 TV equipped with a 63x/1.4N.A. objective. The probe was excited by a LED-based illumination device (OptoLED, Cairn Research) with a 436/20 nm bandpass filter. Donor and acceptor wavelength were separated by a beamsplitter device (Optosplit, Cairn Research) using a 480/40 nm filter for the CFP, a

D505 dichroic mirror and a 535/30 nm filter for the cpVenus. Images were collected with a front-illuminated CCD camera (Photometrics CoolSnap ES2).

Fluorescence ratio and images analysis was calculated in MetaFluor 6.3 software (Universal Imaging). Exposure time and frequency of image capture varied from 100 ms to 300 ms and from 0.5 to 1 Hz, respectively, depending on the intensity of the fluorescent signal of the cells analyzed and on the speed of fluorescence changes.

Mitochondrial membrane potential measurements

To measure mitochondrial membrane potential, we took advantages from Tetra-methyl-rhodamine-Methyl Ester (TMRM) probe. It is membrane permeable and cationic, so it is easily distributed in cellular compartments in base of electrochemical gradients (Scaduto and Grotyohann, 2000). The membrane potential in mitochondrial matrix is negative, around -180mV, this electronegativity induces the TMRM probe to enter, in addition it is an important parameter to evaluate the regulation of some cellular processes like cell death.

- Healthy and patients derived primary fibroblasts were loaded with TMRM probe, 20nM for 30 minutes and then, using a confocal microscope, we evaluated membrane potential alteration after different stimuli (rotenone 4μM, oligomycin 5μM, FCCP 4μM), measuring the probe fluorescence. Changes in mitochondrial membrane potential will cause a redistribution of the dye between mitochondria and cytoplasm.

Data are expressed as percentage relatively the fluorescence measured at basal level.

- Mouse primary cortical neurons at 6 DIV were infected with pEGFP or MCU-GFP Adenovirus, synapsin promoter, for 48 hours. Then, they were loaded with TMRM probe, 20nM for 30 minutes and then, using a confocal microscope, we evaluated membrane potential alteration after excitotoxic stimulus (glutamate 100μM), measuring the probe

fluorescence over time, about 25 minutes. Finally we added a mitochondrial uncoupler (CCCP 10 μM), in order to normalize the fluorescence.

Data are expressed as percentage relatively the fluorescence measured at basal level.

Confocal laser microscope (Zeiss Axiovert 200, objective PlanFluar 40X/1.3) was used. The probe was excited at 560 nm and the emission light was recorded in the 590-650 nm ranges.

ER-mitochondria colocalization

The Split-GFP based technology has been described in (Cabantous et al., 2005). The GFP1-10 fragment targeted to the outer mitochondrial membrane as well as the ER-targeted β-11 strand were kindly provided by Tito Calì (Department of Biology University of Padua). The OMM targeting sequence (VGRNSAIAAGVCGALFIGYCIYFDRKRRSDPN) was taken from the Translocase of Outer Mitochondrial Membrane 20, Tom20. It was expressed as N-terminal tag of GFP1-10 in the pcDNA3 vector. The ER-targeted β-11construct was based on the SAC1, suppressor of actin mutations 1-like protein. The 66 amino acid C-terminal segment of SAC1 (521-587) was directly fused to the β11 strand in the pDEST vector.

Immunofluorescence

- Healthy and mutated primary fibroblasts were grown on 24 mm coverslips. When the cellular confluence was about 70%, the cells were fixed and permeabilized in cold MeOH/Acetone mixture (1:1) for 15 minutes, then blocked in PBS containing 1% BSA, 2% goat serum and 0,3% triton X-100 for 1 hour. Cells were then incubated with primary antibodies, depending on different experiments (anti-LC3antibody 1:200 Cell Signaling; anti-SQSTM1/p62 antibody 1:200 Sigma; anti-Cleaved Caspase3 antibody 1:200 Cell Signaling; anti-Tom20 antibody 1:200 Santa Cruz), overnight at $^{+}$4°C and washed 3 times with PBS. The appropriate isotype matched AlexaFluor conjugated secondary antibodies (Life Technologies)

were used and coverslips were mounted with ProLong Gold Antifade reagent (Life Technologies).

Confocal images were recorded and quantification of the number and the volume of the puncta per cell (for LC3 and SQSTM1/p62 experiments) were performed using ImageJ program.

- Mouse primary cortical neurons were grown on 13 mm glasses coverslips (previously pre-treated with L-poly-lisine) and transfected, after 6 DIV, using Lipofectamine 2000 (see before) with mtRFP as mitochondrial network marker, and with either empty pcDNA vector for control or MCU-flag-pcDNA for the MCU-overexpression (0.2 μg mtRFP : 0.6 μg pcDNA or MCU-flag-pcDNA). The transfection solution was maintained under the cells for 3 hours and then the medium was changed with half of original medium. 24 hours after transfection, primary neurons were fixed with 4% paraformaldeide solution for 20 minutes and permeabilized and blocked in PBS containing 1% BSA, 2% goat serum and 0,3% triton X-100 for 1 hour. Cells were then incubated with primary antibodies, depending on different experiments (anti-flag antibody 1:200 Sigma), overnight at $^{+}$4°C and washed 3 times with PBS. The appropriate isotype matched AlexaFluor conjugated secondary antibodies (Life Technologies) were used and coverslips were mounted with ProLong Gold Antifade reagent (Life Technologies).

- Mouse brain slices 0.4μm were permeabilized and blocked in PBS containing 1% BSA, 2% goat serum and 0,3% triton X-100 for 1 hour in free-floating. Then were incubated with primary antibodies (anti-GFP 1:400 Sigma; anti-TH 1:200 Abcam), overnight at $^{+}$4°C in free-floating and washed 3 times with PBS. The appropriate isotype matched AlexaFluor conjugated secondary antibodies (Life Technologies) were used and coverslips were mounted with VectaSheld (Vector).

Apoptotic counts

Mouse primary cortical neurons were infected at 6 DIV with pEGFP or MCU-GFP Adenovirus, synapsin promoter. Respectively after 48 – 72 – 96 hours after the infection, cells were washed and fixed incubating 4% paraformaldeide solution for 20 minutes. Then, coverslips were mounted with ProLong Gold Antifade reagent (Life Technologies). We took twenty random field of images for condition and then we counted the GFP-positive neurons in the total population, calculating the percentage of fluorescent cells normalized for the number of GFP-positive neurons after 48 hours of infection, which is the one hundred percent value.
In the ideal case, although the total number of neurons could be a little bit reduced over time, the apparent infection efficiency will be maintained.

Stereotaxic injection

Stereotaxic surgery is a minimally invasive form of surgical intervention which makes use of a three-dimensional coordinate system in order to perform injection in different mouse brain's areas.

The specific apparatus for performing brain surgery is characterized from one part to block the mouse braincase by ear bars, in addition the glasses micropipette containing the adenovirus to inject is controlled in the x, y and z planes by the stereotaxic arm. For our injection procedures, thin plastic tubing is attached to the top of the glass micropipette in the holder and a syringe attached to the other end of the plastic tubing is used for virus aspiration or injection (Cetin et al., 2006).

The mice that we used for the surgery are adult C57BL6 strain, around one month of age.

All the mice, before the surgery were intraperitoneally anesthetized using a mixture of ketamine and xylazine in base of their body weight, fixed with ear bars and then the nose clamp connected with gaseous anesthesia were positioned. At this point, using a dissenting

microscope with low magnification, it is possible visualize the mouse skull, perform an incision using surgical scissors in order to keep the area open. Starting from the bregma coordinates, using the stereotaxic arm, it is possible locate the micropipette at the exact x and y coordinates, carefully perforate the skull over the targeted area using a hand-held drill, now starting from the dura, it is possible to evaluate also the z coordinates, when we are in the exact midbrain area, using the micropipette it is possible inject the Adenovirus slowly.

For this experiment we used the synapsin promoter, Adenoviral vector coding either pEGFP alone for control or MCU-GFP for MCU-overexpression. We injected 1μl of stocks virus per mouse, injecting 6.32x10^7 PFU and 4.76x10^7 PFU, respectively of pEGFP and MCU-GFP per mouse.

The exact midbrain stereotaxic coordinates that we have used for our experiments are:

X = -1,3; Y = 3,1; Z = 4,5.

After the Adenovirus injections we have waited 14 days before sacrificing mice, perfusing systemically 4% paraformaldeide solution in order to completely fix all mice tissues. At that point we removed only the brain and sliced it using vibratome obtained 40μm slices.

On the slices we performed an immunofluorescence using anti-GFP antibody, in order to amplify the GFP signal and anti-Tyrosine hydroxylase (anti-TH) antibody in order to detect the dopaminergic neurons.

REFERENCES

Alers, S., Loffler, A.S., Wesselborg, S., and Stork, B. (2012). Role of AMPK-mTOR-Ulk1/2 in the regulation of autophagy: cross talk, shortcuts, and feedbacks. Molecular and cellular biology *32*, 2-11.

Allen, D.G., and Blinks, J.R. (1978). Calcium transients in aequorin-injected frog cardiac muscle. Nature *273*, 509-513.

Andersen, M.N., and Rasmussen, H.B. (2012). AMPK: A regulator of ion channels. Communicative & integrative biology *5*, 480-484.

Ankarcrona, M., Dypbukt, J.M., Bonfoco, E., Zhivotovsky, B., Orrenius, S., Lipton, S.A., and Nicotera, P. (1995). Glutamate-induced neuronal death: a succession of necrosis or apoptosis depending on mitochondrial function. Neuron *15*, 961-973.

Area-Gomez, E., Del Carmen Lara Castillo, M., Tambini, M.D., Guardia-Laguarta, C., de Groof, A.J., Madra, M., Ikenouchi, J., Umeda, M., Bird, T.D., Sturley, S.L., *et al.* (2012). Upregulated function of mitochondria-associated ER membranes in Alzheimer disease. The EMBO journal *31*, 4106-4123.

Baughman, J.M., Perocchi, F., Girgis, H.S., Plovanich, M., Belcher-Timme, C.A., Sancak, Y., Bao, X.R., Strittmatter, L., Goldberger, O., Bogorad, R.L., *et al.* (2011). Integrative genomics identifies MCU as an essential component of the mitochondrial calcium uniporter. Nature *476*, 341-345.

Bayascas, J.R., and Alessi, D.R. (2005). Regulation of Akt/PKB Ser473 phosphorylation. Molecular cell *18*, 143-145.

Berridge, M.J. (1998). Neuronal calcium signaling. Neuron *21*, 13-26.

Berridge, M.J. (2009). Inositol trisphosphate and calcium signalling mechanisms. Biochimica et biophysica acta *1793*, 933-940.

Berridge, M.J., Lipp, P., and Bootman, M.D. (2000). The versatility and universality of calcium signalling. Nature reviews Molecular cell biology *1*, 11-21.

Bezprozvanny, I. (2009). Calcium signaling and neurodegenerative diseases. Trends in molecular medicine *15*, 89-100.

Bjorkoy, G., Lamark, T., Brech, A., Outzen, H., Perander, M., Overvatn, A., Stenmark, H., and Johansen, T. (2005). p62/SQSTM1 forms protein aggregates degraded by autophagy and has a protective effect on huntingtin-induced cell death. The Journal of cell biology *171*, 603-614.

Brandt, U. (2006). Energy converting NADH:quinone oxidoreductase (complex I). Annual review of biochemistry *75*, 69-92.

Brini, M., Marsault, R., Bastianutto, C., Alvarez, J., Pozzan, T., and Rizzuto, R. (1995). Transfected aequorin in the measurement of cytosolic Ca^{2+} concentration ($[Ca^{2+}]c$). A critical evaluation. The Journal of biological chemistry *270*, 9896-9903.

Caballero-Benitez, A., and Moran, J. (2003). Caspase activation pathways induced by staurosporine and low potassium: role of caspase-2. Journal of neuroscience research *71*, 383-396.

Cabantous, S., Terwilliger, T.C., and Waldo, G.S. (2005). Protein tagging and detection with engineered self-assembling fragments of green fluorescent protein. Nature biotechnology *23*, 102-107.

Calcraft, P.J., Ruas, M., Pan, Z., Cheng, X., Arredouani, A., Hao, X., Tang, J., Rietdorf, K., Teboul, L., Chuang, K.T., *et al.* (2009). NAADP mobilizes calcium from acidic organelles through two-pore channels. Nature *459*, 596-600.

Cardenas, C., Miller, R.A., Smith, I., Bui, T., Molgo, J., Muller, M., Vais, H., Cheung, K.H., Yang, J., Parker, I., *et al.* (2010). Essential regulation of cell bioenergetics by constitutive InsP3 receptor Ca^{2+} transfer to mitochondria. Cell *142*, 270-283.

Carriedo, S.G., Yin, H.Z., Sensi, S.L., and Weiss, J.H. (1998). Rapid Ca^{2+} entry through Ca^{2+}-permeable AMPA/Kainate channels triggers marked intracellular Ca^{2+} rises and consequent oxygen radical production. The Journal of neuroscience : the official journal of the Society for Neuroscience *18*, 7727-7738.

Carrol, E.D., Beadsworth, M.B., Jenkins, N., Ratcliffe, L., Ashton, I., Crowley, B., Nye, F.J., and Beeching, N.J. (2006). Clinical and diagnostic findings of an echovirus meningitis outbreak in the north west of England. Postgraduate medical journal *82*, 60-64.

Cetin, A., Komai, S., Eliava, M., Seeburg, P.H., and Osten, P. (2006). Stereotaxic gene delivery in the rodent brain. Nature protocols *1*, 3166-3173.

Chaturvedi, R.K., and Flint Beal, M. (2013). Mitochondrial diseases of the brain. Free radical biology & medicine *63*, 1-29.

Choi, D.W. (1992). Excitotoxic cell death. Journal of neurobiology *23*, 1261-1276.

Choi, D.W., and Koh, J.Y. (1998). Zinc and brain injury. Annual review of neuroscience *21*, 347-375.

Clapham, D.E. (2007). Calcium signaling. Cell *131*, 1047-1058.

Cobbold, P.H., and Bourne, P.K. (1984). Aequorin measurements of free calcium in single heart cells. Nature *312*, 444-446.

Corona, P., Antozzi, C., Carrara, F., D'Incerti, L., Lamantea, E., Tiranti, V., and Zeviani, M. (2001). A novel mtDNA mutation in the ND5 subunit of complex I in two MELAS patients. Annals of neurology *49*, 106-110.

Criollo, A., Maiuri, M.C., Tasdemir, E., Vitale, I., Fiebig, A.A., Andrews, D., Molgo, J., Diaz, J., Lavandero, S., Harper, F., *et al.* (2007). Regulation of autophagy by the inositol trisphosphate receptor. Cell death and differentiation *14*, 1029-1039.

Csordas, G., Renken, C., Varnai, P., Walter, L., Weaver, D., Buttle, K.F., Balla, T., Mannella, C.A., and Hajnoczky, G. (2006). Structural and functional features and significance of the physical linkage between ER and mitochondria. The Journal of cell biology *174*, 915-921.

de Brito, O.M., and Scorrano, L. (2008). Mitofusin 2 tethers endoplasmic reticulum to mitochondria. Nature *456*, 605-610.

De Stefani, D., Raffaello, A., Teardo, E., Szabo, I., and Rizzuto, R. (2011). A forty-kilodalton protein of the inner membrane is the mitochondrial calcium uniporter. Nature *476*, 336-340.

Delivani, P., and Martin, S.J. (2006). Mitochondrial membrane remodeling in apoptosis: an inside story. Cell death and differentiation *13*, 2007-2010.

Deluca, H.F., and Engstrom, G.W. (1961). Calcium uptake by rat kidney mitochondria. Proceedings of the National Academy of Sciences of the United States of America *47*, 1744-1750.

Deter, R.L., and De Duve, C. (1967). Influence of glucagon, an inducer of cellular autophagy, on some physical properties of rat liver lysosomes. The Journal of cell biology *33*, 437-449.

Distelmaier, F., Koopman, W.J., van den Heuvel, L.P., Rodenburg, R.J., Mayatepek, E., Willems, P.H., and Smeitink, J.A. (2009). Mitochondrial complex I deficiency: from organelle dysfunction to clinical disease. Brain *132*, 833-842.

Duchen, M.R. (2004). Mitochondria in health and disease: perspectives on a new mitochondrial biology. Molecular aspects of medicine *25*, 365-451.

Duchen, M.R. (2012). Mitochondria, calcium-dependent neuronal death and neurodegenerative disease. Pflugers Archiv : European journal of physiology *464*, 111-121.

Dyall, S.D., Brown, M.T., and Johnson, P.J. (2004). Ancient invasions: from endosymbionts to organelles. Science *304*, 253-257.

Egan, D.F., Shackelford, D.B., Mihaylova, M.M., Gelino, S., Kohnz, R.A., Mair, W., Vasquez, D.S., Joshi, A., Gwinn, D.M., Taylor, R., *et al.* (2011). Phosphorylation of ULK1 (hATG1) by AMP-activated protein kinase connects energy sensing to mitophagy. Science *331*, 456-461.

Eimerl, S., and Schramm, M. (1994). The quantity of calcium that appears to induce neuronal death. Journal of neurochemistry *62*, 1223-1226.

Frezza, C., Cipolat, S., Martins de Brito, O., Micaroni, M., Beznoussenko, G.V., Rudka, T., Bartoli, D., Polishuck, R.S., Danial, N.N., De Strooper, B., *et al.* (2006). OPA1 controls apoptotic cristae remodeling independently from mitochondrial fusion. Cell *126*, 177-189.

Friberg, H., and Wieloch, T. (2002). Mitochondrial permeability transition in acute neurodegeneration. Biochimie *84*, 241-250.

Fujita, N., Hayashi-Nishino, M., Fukumoto, H., Omori, H., Yamamoto, A., Noda, T., and Yoshimori, T. (2008). An Atg4B mutant hampers the lipidation of LC3 paralogues and causes defects in autophagosome closure. Molecular biology of the cell *19*, 4651-4659.

Garcia-Bustos, J., Heitman, J., and Hall, M.N. (1991). Nuclear protein localization. Biochimica et biophysica acta *1071*, 83-101.

Geisler, S., Holmstrom, K.M., Skujat, D., Fiesel, F.C., Rothfuss, O.C., Kahle, P.J., and Springer, W. (2010). PINK1/Parkin-mediated mitophagy is dependent on VDAC1 and p62/SQSTM1. Nature cell biology *12*, 119-131.

Gibson, G.E., Starkov, A., Blass, J.P., Ratan, R.R., and Beal, M.F. (2010). Cause and consequence: mitochondrial dysfunction initiates and propagates neuronal dysfunction, neuronal death and behavioral abnormalities in age-associated neurodegenerative diseases. Biochimica et biophysica acta *1802*, 122-134.

Gomes, L.C., Di Benedetto, G., and Scorrano, L. (2011). During autophagy mitochondria elongate, are spared from degradation and sustain cell viability. Nature cell biology *13*, 589-598.

Gordon, P.B., Holen, I., Fosse, M., Rotnes, J.S., and Seglen, P.O. (1993). Dependence of hepatocytic autophagy on intracellularly sequestered calcium. The Journal of biological chemistry *268*, 26107-26112.

Granatiero, V., Patron, M., Tosatto, A., Merli, G., and Rizzuto, R. (2014). Using targeted variants of aequorin to measure Ca^{2+} levels in intracellular organelles. Cold Spring Harbor protocols *2014*.

Hajnoczky, G., Csordas, G., Das, S., Garcia-Perez, C., Saotome, M., Sinha Roy, S., and Yi, M. (2006). Mitochondrial calcium signalling and cell death: approaches for assessing the role of mitochondrial Ca^{2+} uptake in apoptosis. Cell calcium *40*, 553-560.

Hajnoczky, G., Robb-Gaspers, L.D., Seitz, M.B., and Thomas, A.P. (1995). Decoding of cytosolic calcium oscillations in the mitochondria. Cell *82*, 415-424.

Hanada, T., Satomi, Y., Takao, T., and Ohsumi, Y. (2009). The amino-terminal region of Atg3 is essential for association with phosphatidylethanolamine in Atg8 lipidation. FEBS letters *583*, 1078-1083.

Hara, K., Maruki, Y., Long, X., Yoshino, K., Oshiro, N., Hidayat, S., Tokunaga, C., Avruch, J., and Yonezawa, K. (2002). Raptor, a binding partner of target of rapamycin (TOR), mediates TOR action. Cell *110*, 177-189.

Hardie, D.G. (2007). AMP-activated/SNF1 protein kinases: conserved guardians of cellular energy. Nature reviews Molecular cell biology *8*, 774-785.

Hartl, F.U., Pfanner, N., Nicholson, D.W., and Neupert, W. (1989). Mitochondrial protein import. Biochimica et biophysica acta *988*, 1-45.

Hartley, D.M., Kurth, M.C., Bjerkness, L., Weiss, J.H., and Choi, D.W. (1993). Glutamate receptor-induced $45Ca^{2+}$ accumulation in cortical cell culture correlates with subsequent neuronal degeneration. The Journal of neuroscience : the official journal of the Society for Neuroscience *13*, 1993-2000.

He, T.C., Zhou, S., da Costa, L.T., Yu, J., Kinzler, K.W., and Vogelstein, B. (1998). A simplified system for generating recombinant adenoviruses. Proceedings of the National Academy of Sciences of the United States of America *95*, 2509-2514.

Head, J.F., Inouye, S., Teranishi, K., and Shimomura, O. (2000). The crystal structure of the photoprotein aequorin at 2.3 A resolution. Nature *405*, 372-376.

Hoeflich, K.P., and Ikura, M. (2002). Calmodulin in action: diversity in target recognition and activation mechanisms. Cell *108*, 739-742.

Inouye, S., and Tsuji, F.I. (1993). Cloning and sequence analysis of cDNA for the $Ca(^{2+})$-activated photoprotein, clytin. FEBS letters *315*, 343-346.

Jiang, D., Zhao, L., and Clapham, D.E. (2009). Genome-wide RNAi screen identifies Letm1 as a mitochondrial Ca^{2+}/H+ antiporter. Science *326*, 144-147.

Jung, C.H., Ro, S.H., Cao, J., Otto, N.M., and Kim, D.H. (2010). mTOR regulation of autophagy. FEBS letters *584*, 1287-1295.

Kim, I., Rodriguez-Enriquez, S., and Lemasters, J.J. (2007). Selective degradation of mitochondria by mitophagy. Archives of biochemistry and biophysics *462*, 245-253.

Kim, J., Kundu, M., Viollet, B., and Guan, K.L. (2011). AMPK and mTOR regulate autophagy through direct phosphorylation of Ulk1. Nature cell biology *13*, 132-141.

Kirichok, Y., Krapivinsky, G., and Clapham, D.E. (2004). The mitochondrial calcium uniporter is a highly selective ion channel. Nature *427*, 360-364.

Klionsky, D.J. (2007). Autophagy: from phenomenology to molecular understanding in less than a decade. Nature reviews Molecular cell biology *8*, 931-937.

Klionsky, D.J., Abdalla, F.C., Abeliovich, H., Abraham, R.T., Acevedo-Arozena, A., Adeli, K., Agholme, L., Agnello, M., Agostinis, P., Aguirre-Ghiso, J.A., *et al.* (2012). Guidelines for the use and interpretation of assays for monitoring autophagy. Autophagy *8*, 445-544.

Klionsky, D.J., and Ohsumi, Y. (1999). Vacuolar import of proteins and organelles from the cytoplasm. Annual review of cell and developmental biology *15*, 1-32.

Koppen, M., and Langer, T. (2007). Protein degradation within mitochondria: versatile activities of AAA proteases and other peptidases. Critical reviews in biochemistry and molecular biology *42*, 221-242.

Kuma, A., Hatano, M., Matsui, M., Yamamoto, A., Nakaya, H., Yoshimori, T., Ohsumi, Y., Tokuhisa, T., and Mizushima, N. (2004). The role of autophagy during the early neonatal starvation period. Nature *432*, 1032-1036.

Levine, B., and Kroemer, G. (2008). Autophagy in the pathogenesis of disease. Cell *132*, 27-42.

Mallilankaraman, K., Doonan, P., Cardenas, C., Chandramoorthy, H.C., Muller, M., Miller, R., Hoffman, N.E., Gandhirajan, R.K., Molgo, J., Birnbaum, M.J., *et al.* (2012). MICU1 is an essential gatekeeper for MCU-mediated mitochondrial Ca($^{2+}$) uptake that regulates cell survival. Cell *151*, 630-644.

Mannella, C.A. (2006). Structure and dynamics of the mitochondrial inner membrane cristae. Biochimica et biophysica acta *1763*, 542-548.

Martinou, I., Desagher, S., Eskes, R., Antonsson, B., Andre, E., Fakan, S., and Martinou, J.C. (1999). The release of cytochrome c from mitochondria during apoptosis of NGF-deprived sympathetic neurons is a reversible event. The Journal of cell biology *144*, 883-889.

Massey, A.C., Zhang, C., and Cuervo, A.M. (2006). Chaperone-mediated autophagy in aging and disease. Current topics in developmental biology *73*, 205-235.

Matsui, Y., Takagi, H., Qu, X., Abdellatif, M., Sakoda, H., Asano, T., Levine, B., and Sadoshima, J. (2007). Distinct roles of autophagy in the heart during ischemia and reperfusion: roles of AMP-activated protein kinase and Beclin 1 in mediating autophagy. Circulation research *100*, 914-922.

McCormack, J.G., Halestrap, A.P., and Denton, R.M. (1990). Role of calcium ions in regulation of mammalian intramitochondrial metabolism. Physiological reviews *70*, 391-425.

Meldolesi, J., and Pozzan, T. (1998). The endoplasmic reticulum Ca^{2+} store: a view from the lumen. Trends in biochemical sciences *23*, 10-14.

Melendez-Hevia, E., Waddell, T.G., and Cascante, M. (1996). The puzzle of the Krebs citric acid cycle: assembling the pieces of chemically feasible reactions, and opportunism in the design of metabolic pathways during evolution. Journal of molecular evolution *43*, 293-303.

Mitchell, P. (1967). Proton current flow in mitochondrial systems. Nature *214*, 1327-1328.

Mizushima, N., and Klionsky, D.J. (2007). Protein turnover via autophagy: implications for metabolism. Annual review of nutrition *27*, 19-40.

Mizushima, N., Yoshimori, T., and Levine, B. (2010). Methods in mammalian autophagy research. Cell *140*, 313-326.

Montero, M., Alonso, M.T., Carnicero, E., Cuchillo-Ibanez, I., Albillos, A., Garcia, A.G., Garcia-Sancho, J., and Alvarez, J. (2000). Chromaffin-cell stimulation triggers fast millimolar mitochondrial Ca^{2+} transients that modulate secretion. Nature cell biology *2*, 57-61.

Montero, M., Brini, M., Marsault, R., Alvarez, J., Sitia, R., Pozzan, T., and Rizzuto, R. (1995). Monitoring dynamic changes in free Ca^{2+} concentration in the endoplasmic reticulum of intact cells. The EMBO journal *14*, 5467-5475.

Narendra, D., Tanaka, A., Suen, D.F., and Youle, R.J. (2008). Parkin is recruited selectively to impaired mitochondria and promotes their autophagy. The Journal of cell biology *183*, 795-803.

Nicholls, D.G. (2005). Mitochondria and calcium signaling. Cell calcium *38*, 311-317.

Norenberg, M.D., and Rao, K.V. (2007). The mitochondrial permeability transition in neurologic disease. Neurochemistry international *50*, 983-997.

Nothwehr, S.F., and Gordon, J.I. (1990). Targeting of proteins into the eukaryotic secretory pathway: signal peptide structure/function relationships. BioEssays : news and reviews in molecular, cellular and developmental biology *12*, 479-484.

Olney, J.W., and Sharpe, L.G. (1969). Brain lesions in an infant rhesus monkey treated with monsodium glutamate. Science *166*, 386-388.

Orrenius, S., and Nicotera, P. (1994). The calcium ion and cell death. Journal of neural transmission Supplementum *43*, 1-11.

Orrenius, S., Zhivotovsky, B., and Nicotera, P. (2003). Regulation of cell death: the calcium-apoptosis link. Nature reviews Molecular cell biology *4*, 552-565.

Palmer, A.E., and Tsien, R.Y. (2006). Measuring calcium signaling using genetically targetable fluorescent indicators. Nature protocols *1*, 1057-1065.

Palty, R., Silverman, W.F., Hershfinkel, M., Caporale, T., Sensi, S.L., Parnis, J., Nolte, C., Fishman, D., Shoshan-Barmatz, V., Herrmann, S., *et al.* (2010). NCLX is an essential

component of mitochondrial Na+/Ca^{2+} exchange. Proceedings of the National Academy of Sciences of the United States of America *107*, 436-441.

Patron, M.D.S., D.; Checchetto, V.; Raffaello, A.; Teardo, E.; Vecellio-Reane, D.; Mantoan, M.; Granatiero, V.; Szabò, I.; Rizzuto, R. (2014). MICU1 and MICU2 finely tune the mitochondrial Ca^{2+} uniporter by exerting opposite

effect on MCU activity. MOLECULAR-CELL *in press*.

Pattingre, S., Tassa, A., Qu, X., Garuti, R., Liang, X.H., Mizushima, N., Packer, M., Schneider, M.D., and Levine, B. (2005). Bcl-2 antiapoptotic proteins inhibit Beclin 1-dependent autophagy. Cell *122*, 927-939.

Pereira, C.F., and Oliveira, C.R. (2000). Oxidative glutamate toxicity involves mitochondrial dysfunction and perturbation of intracellular Ca^{2+} homeostasis. Neuroscience research *37*, 227-236.

Perocchi, F., Gohil, V.M., Girgis, H.S., Bao, X.R., McCombs, J.E., Palmer, A.E., and Mootha, V.K. (2010). MICU1 encodes a mitochondrial EF hand protein required for Ca($^{2+}$) uptake. Nature *467*, 291-296.

Pinton, P., Pozzan, T., and Rizzuto, R. (1998). The Golgi apparatus is an inositol 1,4,5-trisphosphate-sensitive Ca^{2+} store, with functional properties distinct from those of the endoplasmic reticulum. The EMBO journal *17*, 5298-5308.

Pinton, P., Rimessi, A., Romagnoli, A., Prandini, A., and Rizzuto, R. (2007). Biosensors for the detection of calcium and pH. Methods in cell biology *80*, 297-325.

Pinton, P., and Rizzuto, R. (2006). Bcl-2 and Ca^{2+} homeostasis in the endoplasmic reticulum. Cell death and differentiation *13*, 1409-1418.

Pivovarova, N.B., and Andrews, S.B. (2010). Calcium-dependent mitochondrial function and dysfunction in neurons. The FEBS journal *277*, 3622-3636.

Pivovarova, N.B., Hongpaisan, J., Andrews, S.B., and Friel, D.D. (1999). Depolarization-induced mitochondrial Ca accumulation in sympathetic neurons: spatial and temporal characteristics. The Journal of neuroscience : the official journal of the Society for Neuroscience *19*, 6372-6384.

Pozzan, T., and Rizzuto, R. (2000). High tide of calcium in mitochondria. Nature cell biology *2*, E25-27.

Qiu, J., Tan, Y.W., Hagenston, A.M., Martel, M.A., Kneisel, N., Skehel, P.A., Wyllie, D.J., Bading, H., and Hardingham, G.E. (2013). Mitochondrial calcium uniporter Mcu controls excitotoxicity and is transcriptionally repressed by neuroprotective nuclear calcium signals. Nature communications *4*, 2034.

Rasola, A., and Bernardi, P. (2011). Mitochondrial permeability transition in Ca($^{2+}$)-dependent apoptosis and necrosis. Cell calcium *50*, 222-233.

Ravikumar, B., Sarkar, S., Davies, J.E., Futter, M., Garcia-Arencibia, M., Green-Thompson, Z.W., Jimenez-Sanchez, M., Korolchuk, V.I., Lichtenberg, M., Luo, S., *et al.* (2010). Regulation of mammalian autophagy in physiology and pathophysiology. Physiological reviews *90*, 1383-1435.

Rizzuto, R. (2003). Calcium mobilization from mitochondria in synaptic transmitter release. The Journal of cell biology *163*, 441-443.

Rizzuto, R., Brini, M., Murgia, M., and Pozzan, T. (1993). Microdomains with high Ca^{2+} close to IP3-sensitive channels that are sensed by neighboring mitochondria. Science *262*, 744-747.

Rizzuto, R., De Stefani, D., Raffaello, A., and Mammucari, C. (2012). Mitochondria as sensors and regulators of calcium signalling. Nature reviews Molecular cell biology *13*, 566-578.

Rizzuto, R., Pinton, P., Carrington, W., Fay, F.S., Fogarty, K.E., Lifshitz, L.M., Tuft, R.A., and Pozzan, T. (1998). Close contacts with the endoplasmic reticulum as determinants of mitochondrial Ca^{2+} responses. Science *280*, 1763-1766.

Rizzuto, R., and Pozzan, T. (2006). Microdomains of intracellular Ca^{2+}: molecular determinants and functional consequences. Physiological reviews *86*, 369-408.

Rizzuto, R., Simpson, A.W., Brini, M., and Pozzan, T. (1992). Rapid changes of mitochondrial Ca^{2+} revealed by specifically targeted recombinant aequorin. Nature *358*, 325-327.

Sandoval, H., Thiagarajan, P., Dasgupta, S.K., Schumacher, A., Prchal, J.T., Chen, M., and Wang, J. (2008). Essential role for Nix in autophagic maturation of erythroid cells. Nature *454*, 232-235.

Sarkar, S., Floto, R.A., Berger, Z., Imarisio, S., Cordenier, A., Pasco, M., Cook, L.J., and Rubinsztein, D.C. (2005). Lithium induces autophagy by inhibiting inositol monophosphatase. The Journal of cell biology *170*, 1101-1111.

Scaduto, R.C., Jr., and Grotyohann, L.W. (2000). 2,3-butanedione monoxime unmasks $Ca(^{2+})$-induced NADH formation and inhibits electron transport in rat hearts. American journal of physiology Heart and circulatory physiology *279*, H1839-1848.

Scorrano, L., Ashiya, M., Buttle, K., Weiler, S., Oakes, S.A., Mannella, C.A., and Korsmeyer, S.J. (2002). A distinct pathway remodels mitochondrial cristae and mobilizes cytochrome c during apoptosis. Developmental cell *2*, 55-67.

Sekulic, A., Hudson, C.C., Homme, J.L., Yin, P., Otterness, D.M., Karnitz, L.M., and Abraham, R.T. (2000). A direct linkage between the phosphoinositide 3-kinase-AKT signaling pathway and the mammalian target of rapamycin in mitogen-stimulated and transformed cells. Cancer research *60*, 3504-3513.

Sou, Y.S., Waguri, S., Iwata, J., Ueno, T., Fujimura, T., Hara, T., Sawada, N., Yamada, A., Mizushima, N., Uchiyama, Y., *et al.* (2008). The Atg8 conjugation system is indispensable for proper development of autophagic isolation membranes in mice. Molecular biology of the cell *19*, 4762-4775.

Starkov, A.A., Chinopoulos, C., and Fiskum, G. (2004). Mitochondrial calcium and oxidative stress as mediators of ischemic brain injury. Cell calcium *36*, 257-264.

Suen, D.F., Narendra, D.P., Tanaka, A., Manfredi, G., and Youle, R.J. (2010). Parkin overexpression selects against a deleterious mtDNA mutation in heteroplasmic cybrid cells. Proceedings of the National Academy of Sciences of the United States of America *107*, 11835-11840.

Trenker, M., Malli, R., Fertschai, I., Levak-Frank, S., and Graier, W.F. (2007). Uncoupling proteins 2 and 3 are fundamental for mitochondrial Ca^{2+} uniport. Nature cell biology *9*, 445-452.

Tsukada, M., and Ohsumi, Y. (1993). Isolation and characterization of autophagy-defective mutants of Saccharomyces cerevisiae. FEBS letters *333*, 169-174.

Valsecchi, F., Esseling, J.J., Koopman, W.J., and Willems, P.H. (2009). Calcium and ATP handling in human NADH:ubiquinone oxidoreductase deficiency. Biochim Biophys Acta *1792*, 1130-1137.

Valsecchi, F., Koopman, W.J., Manjeri, G.R., Rodenburg, R.J., Smeitink, J.A., and Willems, P.H. (2010). Complex I disorders: causes, mechanisms, and development of treatment strategies at the cellular level. Developmental disabilities research reviews *16*, 175-182.

Varabyova, A., Stojanovski, D., and Chacinska, A. (2013). Mitochondrial protein homeostasis. IUBMB life *65*, 191-201.

Vogel, R.O., Smeitink, J.A., and Nijtmans, L.G. (2007). Human mitochondrial complex I assembly: a dynamic and versatile process. Biochimica et biophysica acta *1767*, 1215-1227.

Wang, C.W., and Klionsky, D.J. (2003). The molecular mechanism of autophagy. Molecular medicine *9*, 65-76.

Ward, M.W., Rego, A.C., Frenguelli, B.G., and Nicholls, D.G. (2000). Mitochondrial membrane potential and glutamate excitotoxicity in cultured cerebellar granule cells. The Journal of neuroscience : the official journal of the Society for Neuroscience *20*, 7208-7219.

Wasilewski, M., Semenzato, M., Rafelski, S.M., Robbins, J., Bakardjiev, A.I., and Scorrano, L. (2012). Optic atrophy 1-dependent mitochondrial remodeling controls steroidogenesis in trophoblasts. Current biology : CB *22*, 1228-1234.

Willems, P.H., Smeitink, J.A., and Koopman, W.J. (2009). Mitochondrial dynamics in human NADH:ubiquinone oxidoreductase deficiency. Int J Biochem Cell Biol *41*, 1773-1782.

Willems, P.H., Valsecchi, F., Distelmaier, F., Verkaart, S., Visch, H.J., Smeitink, J.A., and Koopman, W.J. (2008). Mitochondrial Ca^{2+} homeostasis in human NADH:ubiquinone oxidoreductase deficiency. Cell Calcium *44*, 123-133.

Wong, P.M., Puente, C., Ganley, I.G., and Jiang, X. (2013). The ULK1 complex: sensing nutrient signals for autophagy activation. Autophagy *9*, 124-137.

Zeviani, M., and Antozzi, C. (1997). Mitochondrial disorders. Molecular human reproduction *3*, 133-148.

Zeviani, M., and Carelli, V. (2003). Mitochondrial disorders. Current opinion in neurology *16*, 585-594.

Zeviani, M., and Di Donato, S. (2004). Mitochondrial disorders. Brain : a journal of neurology *127*, 2153-2172.

Zhang, Y., Qi, H., Taylor, R., Xu, W., Liu, L.F., and Jin, S. (2007). The role of autophagy in mitochondria maintenance: characterization of mitochondrial functions in autophagy-deficient S. cerevisiae strains. Autophagy *3*, 337-346.